Astronomy & Astrophysics manuscript no. n7603 November 1, 2018
(DOI: will be inserted by hand later)

The field surrounding NGC 7603: cosmological or non-cosmological redshifts?

M. López-Corredoira[1] and C. M. Gutiérrez[2]

[1] Astronomisches Institut der Universität Basel. Venusstrasse 7. CH-4102 Binningen, Switzerland

[2] Instituto de Astrofísica de Canarias, E-38205 La Laguna, Tenerife, Spain

Received xxxx / Accepted xxxx

Abstract. We present new observations of the field surrounding the Seyfert galaxy NGC 7603, where four galaxies with different redshifts—NGC 7603 ($z = 0.029$), NGC 7603B ($z = 0.057$) and two fainter emission line galaxies ($z = 0.245$ and $z = 0.394$)—are apparently connected by a narrow filament, leading to a possible case of anomalous redshift. The observations comprise broad and narrow band imaging and intermediate resolution spectroscopy of some of the objects in the field. The new data confirm the redshift of the two emission-line objects found within the filament connecting NGC 7603 and NGC 7603B, and settles their type with better accuracy . Although both objects are point-like in ground based images, using HST archive images we show that the objects have structure with a FWHM=0.3-0.4 arcsec. The photometry in the R-band obtained during three different campaigns spread over two years does not show any signs of variability in these objects above $0.3 - 0.4$ mag. All the above information and the relative strength and width of the main spectral lines allow us to classify these as HII galaxies with very vigorous star formation, while the rest of the filament and NGC 7603B lack star formation. We delineate the halo of NGC 7603 out to 26.2 mag/arcsec^2 in the Sloan r band filter and find evidence for strong internal distortions. New narrow emission line galaxies at z=0.246, 0.117 and 0.401 are also found at respectively 0.8, 1.5 and 1.7 arcmin to the West of the filament within the fainter contour of this halo. We have studied the spatial distribution of objects in the field within 1.5 arcmin of NGC 7603. We conclude that the density of QSOs is roughly within the expected value of the limiting magnitude of our observations. However, the configuration of the four galaxies apparently connected by the filament appears highly unusual. The probability of three background galaxies of any type with apparent B-magnitudes up to 16.6, 21.1 and 22.1 (the observed magnitudes, extinction correction included) being randomly projected on the filament

of the fourth galaxy (NGC 7603) is computed resulting $\approx 3 \times 10^{-9}$. Furthermore, the possible detection of very vigorous star formation observed in the HII galaxies of the filament would have a low probability if they were background normal-giant galaxies; instead, the intensity of the lines is typical of dwarf HII galaxies. Hence, a set of coincidences with a very low probability would be necessary to explain this as a fortuitous projection of background sources. Several explanations in terms of cosmological or non-cosmological redshifts are discussed.

Key words. Galaxies: individual: NGC 7603 — Galaxies: statistics — Galaxies: peculiar — Galaxies: starburst — distance scale

1. Introduction

1.1. Anomalous redshift problem

The problem of the apparent optical associations of galaxies with very different redshifts, the so-called anomalous redshifts (Narlikar 1989; Arp 1987, 1998), is old but still alive. Although surprisingly ignored by most of the astronomical community, there is increasing evidence of examples of such anomalies. Statistical evidence has grown for such associations over the last 30 years (Burbidge 1996, 2001). For instance, all non-elliptical galaxies brighter than 12.8 mag with apparent companion galaxies have been examined (Arp 1981), and 13 of the 34 candidate companion galaxies were found to have QSOs with higher redshift. Given an accidental probability of less than 0.01 per galaxy, the global probability of this to be a chance is $\sim 10^{-17}$. Bias effects alone cannot be responsible for these correlations (Burbidge 2001; Hoyle & Burbidge 1996; Benítez et al. 2001). Weak gravitational lensing by dark matter has been proposed (Gott & Gunn 1974; Schneider 1989; Wu 1996; Burbidge et al. 1997) as the cause of these correlations, although this seems to be insufficient to explain them (Burbidge et al. 1997; Burbidge 2001; Benítez et al. 2001; Gaztañaga 2003; Jain et al. 2003), and cannot work at all for the correlations with the brightest and nearest galaxies. The statistical relevance of these associations is still currently a matter of debate (Sluse et al. 2003).

A recent compilation of associations galaxies−QSOs has been presented by Burbidge (1996). Some remarkable cases of apparent associations between objects with different redshift are Arp 220 (Ohyama et al. 1999; Arp et al. 2001), NGC 1068 (Burbidge 1999a; Bell 2002a), NGC 3067 (Carilli et al. 1989; Carilli & van Gorkom 1992), NGC 3628 (Arp et al. 2002), NGC 4258 (Pietsch et al. 1994; Kondratko et al. 2001), NGC 4319 (Sulentic & Arp 1987), etc. Some of these may be just fortuitous cases in which background objects are close to the foreground galaxy, although the statistical mean correlations remain to

Send offprint requests to: cgc@ll.iac.es

be explained, and some cases alone have very small probability to be a projection of background objects.

Associations of galaxies with different redshifts might also take place: forty-three systems among the hundred Hickson (1982) groups of galaxies (compact groups of galaxies containing four to six members) have one redshift very different from the mean of the others (Sulentic 1997). For instance, Stephan's quintet (Moles et al. 1998; Gutiérrez et al. 2002), the chain VV172 (Arp 1987; Narlikar 1989), etc. Although the numbers, sizes, magnitudes and morphological types of the discordant redshift members might agree with a scenario of chance projections, the distribution of positions in quintets is more centrally concentrated than expected in such a scenario (Mendes de Oliveira 1995). This author claims that compact groups might act as gravitational lenses and therefore explain the difference in concentration, but this remains to be justified.

To explain these associations Hoyle et al. (1993) proposed new physics in which part of the measured redshifs are not caused by the expansion of the Universe. Other theories have been proposed too (see §5.3). We are carrying out a series of observations of some of the suspicious systems in order to know more about them and to throw further light to the problem (Gutiérrez et al. 2002; López-Corredoira & Gutiérrez 2002; Gutiérrez & López-Corredoira 2003 in preparation; and this paper). In particular, this paper is about the system of NGC 7603 and the surrounding objects.

1.2. NGC 7603

The main galaxy, NGC 7603, is a broad line Seyfert I galaxy with z= 0.0295 and B = 14.04 mag (de Vaucouleurs et al. 1991). This galaxy has been studied mainly in relation to its variability, which was discovered by Kopylov et al. (1974), and Tohline & Osterbrock (1976). Kollatschny et al. (2000) have presented the results of an extensive programme to study the line and continuum variability over a period of twenty years. They detected spectral variations on timescales from months to years. The variability observed is 5−10 in the intensity in the Balmer and Helium lines, and in the continuum. From the perspective of the Eigenvector 1 parameter space for AGNs (Sulentic et al. 2000, 2002), the Balmer lines are unusually broad and show a very complex structure. The Balmer lines are blueshifted relative to the local 'rest frame' of the AGN by between 1000 and 2000 km/s. Less than 5% of AGN show such characteristics. Such lines are more common in radio-loud quasars, where one sees ejected synchrotron lobes. It shows unusually strong FeII emission for an AGN with such broad lines (Goodrich 1989, Kollatschny et al. 2000).

The system around NGC 7603 is very interesting because it is among the cases (Arp 1980) with some filamentary structure joining galaxies with different redshift. Arp (1971, 1975, 1980) has claimed that the compact member has somehow been ejected from the bigger object. NGC 7603 and its filament are so distorted that significant tidal dis-

turbance can be reasonably assumed, without a clear candidate for companion galaxy producing the tides (see §3.1). Another fact that has attracted attention (Arp 1971, 1975; Sharp 1986) is the proximity of NGC 7603B, a spiral galaxy with higher redshift (z= 0.0569) located 59 arcseconds to the SE of NGC 7603. The angular proximity of both galaxies and the apparently luminous connection between them has converted the system into an important example of an anomalous redshift association. Hoyle (1972) has pointed out that NGC 7603 is one of the most strange cases, and which needs a non-standard theory to be explained. Apart from the above facts there are also two in principle point-like objects superimposed on the filament that apparently connects both galaxies. We thought that the particularities of the systems deserve more attention and decided to study the bridge and the point-like objects mentioned.

In López-Corredoira & Gutiérrez (2002, hereafter Paper I) we presented intermediate resolution spectra of the filament and the two objects mentioned (see Fig. 1 of Paper I). From several absorption lines we estimated the redshift of the filament apparently connecting NGC 7603 and NGC 7603B as z= 0.030, very similar to the redshift of NGC 7603 and probably associated with this galaxy. We identified several emission lines in the spectra of the two knots and from the emission lines of Hβ, OII (3727Å) and OIII (4959 and 5007 Å) we determined their redshifts, obtaining 0.39 and 0.24 for the objects closer and farther from NGC 7603 respectively. The two objects might be QSOs or HII-galaxies. The spectra of paper I had not enough resolution to determine their nature definitively (since we used a wide slit) and the seeing conditions limited the possibility of seeing structure under 1 arcsecond in these objects. These intriguing results motivated us to continue with the study of this system. We planned new observations with the aim of answering the following questions: i) What is the nature of the two knots in the filament?, ii) Are there any other high redshift objects in the halo surrounding NGC 7603?, and iii) Are there any clues in the surrounding field that help us understand the nature of this apparent association?

This paper contains the analysis of new observations and is structured as follows: Section 2 presents the details of the observations and data reduction. Section 3 presents the observed images, and the main features discovered in each component. Section 4 presents the spectroscopy of some sources. Section 5 calculates the probabilities of the observed configuration to be an accidental projection of background galaxies, and discusses the results presenting some possible physical scenarios to explain them. A summary with the main results is given in Section 6.

Table 1. Observations.

Telescope and instrument	Epoch	Mode	Exposure time	Seeing
IAC80 (0.8 m) CCD	Jul.8-00/Aug.17-01	Image, narrow-fi.IAC39-6767 Å	30000 s (dark)	1.8”
	Aug.6-00/Jul.22,Aug.15-01	Image, narrow-fi.IAC35-6931 Å	52834 s (grey)	1.8”
NOT (2.6 m) ALFOSC	2000 June 13	Image, narrow-fi.IAC39-6767 Å	900 s (dark)	1”
	2000 June 13	Image, narrow-fi.IAC35-6931 Å	900 s (bright)	1”
	2000 June 13	Image, R-Bessel band	900 s (dark)	1”
	3001 August 12	Image, R-Bessel band	300 s (dark)	1.5”-2.0”
	2002 November 30	Image, R-Bessel band	900 s (dark)	1.5”-2.0”
	2002 November 30	Image, u-Sloan band	3200 s (dark)	1.5”-2.0”
	2002 November 30	Image, g-Sloan band	1200 s (dark)	1.5”-2.0”
	2002 November 30	Image, i-Sloan band	900 s (dark)	1.5”-2.0”
	2002 December 2	Image, r-Sloan band	1200 s (non-phot.)	1.5”-2.0”
	2002 December 3	Image, r-Sloan band	4200 s (dark)	1.5”-2.0”
(only Paper I) $--->$	August 12, 2001	Spectr.l.slit, gr.#4, ap.5”	14225 s (dark)	1.5”-2.0”
WHT (4.2 m) ISIS red arm	2002 December 28	Spectr.l.slit, gr.R158R, ap.1.2”	5400 s (Pos 1)	—
	2002 December 29	Spectr.l.slit, gr.R158R, ap.1.5”	5400 s (Pos 2)	—
	2002 December 29 2002	Spectr.l.slit, gr.R158R, ap.1.5”	1800 s (Pos 3)	—
HST WFPC2	1994 July 3	Image, filter F606W	500 s.	—

2. Observations

The observations presented here comprise narrow and broad band imaging, and spectroscopy with intermediate resolution. These observations were taken at the IAC80[1], NOT[2], WHT[3] telescopes, and from the HST archive[4]. Table 1 presents a summary of the observations.

We wanted to check for the presence of Hα emission in the filament connecting NGC 7603 and NGC 7603B as well as in the galaxies themselves. NII (6583 Å) is also interesting and might be stronger if e.g. shocks were involved; it would be observed in narrow filters of FWHM 50 Å centered at Hα emission. During several campaigns in 2000 and 2001

[1] The telescope is at the Spanish Teide Observatory on the island of Tenerife and is operated by the Instituto de Astrofísica de Canarias

[2] The Nordic Optical Telescope (NOT) is operated on the island of La Palma jointly by Denmark, Finland, Iceland, Norway, and Sweden, in the Spanish Observatorio del Roque de los Muchachos of the Instituto de Astrofísica de Canarias.

[3] The William Herschel Telescope (WHT) is operated on the island of La Palma by the Isaac Newton Group of Telescopes.

[4] Based on observations made with the NASA/ESA Hubble Space Telescope, obtained from the data archive at the Space Telescope Science Institute. STScI is operated by the Association of Universities for Research in Astronomy, Inc. under NASA contract NAS 5-26555.

we obtained imaging at the IAC80 and NOT with the IAC39 and IAC35 filters which are centred on 6767 and 6931 Å and which match the Hα line at velocities of 9,372 and 16,870 km s^{-1} respectively and have a FWHM equivalent to 2,000 km s^{-1}. These ranges in velocity correspond to the redshifts of NGC 7603 and NGC 7603B respectively. The images were reduced using a standard procedure that comprises bias subtraction, flat-field correction, shifting and co-addition of individual exposures. The continuum in each case was subtracted using a resampled and scaled image (in order to have the same resolution of the IAC80: 0.435 arcsec pixel^{-1}) in the R band taken on 2000 June 13th at the NOT.

With the broad band images we wanted to delineate in detail the halo of the system NGC 7603 - NGC 7603B, to detect other possible candidates in the field and measure their colours, and to constrain possible variability of the two objects in the filament. For the study of the variability we took several images in the R band (Bessel) in the period 2000-2002. For the remaining tasks, apart from the R filter, we observed the field with the Sloan u, g, r, and i filters. In all cases we used the NOT with the ALFOSC instrument. The images were reduced following the standard procedure mentioned above. The conditions were photometric in all runs except on December 2. For the 2000 June 13th observation, several Landolt calibration fields (Landolt 1992) were observed. The observations in the other two runs with the R filter at the NOT (2001 August 12th and 2002 November 30) were relative calibrated with respect to this using using eight stars in the field. For the Sloan filters, we have calibrated with some stars from the list given by Smith et al. (2002).

Because of limiting atmospheric conditions, we could not see details below 1 arcsec resolution from the ground telescopes images. Therefore, Hubble Space Telescope archive were also used to obtain a high spatial resolution of the objects embedded in the filament. These data come from the HST Proposal 5479 made by Matthew Malkan, which was used to produce the paper Malkan et al. (1998). The image, although less deep (exposure time: 500 s.), allows us to see small scale details of some interesting objects, since this includes the filament connecting NGC 7603 and NGC 7603B.

We obtained spectroscopy in two campaigns, the first at the NOT using ALFOSC (presented in Paper I and not considered here) and the second nearly a year and a half later using ISIS at the WHT in order to get further and better spectra than in Paper I and to study other objects in the field. At the WHT we put the slit in three different positions to optimize the observation of the objects within the filament and several other objects that were selected according to their colours (see §3.2). The grism used was R158R. We took Tungsten, and Cu-Ne and Cu-Ar calibration lamps for flat-field correction and spectral calibration respectively. The data were bias subtracted. After some tests we decided not apply any flat fielding correction because such corrections would require prohibitive exposure times with the Tungsten lamp on the blue side of the spectrum

and in any case this correction is very small ($\sim 1\%$) in the red part of the spectrum. The FWHM measured of the lines is 8 Å for the first position, and 20 Å for the second and third position. We extracted the spectra using the task *apall* of IRAF[5]. The data are sampled at 1.62 Å/pixel and covers from 2810 Å to 10450 Å. However, due to the response of the grism, the sensitivity of the first 1000 pixels (below 4400 Å) or the last 700 pixels (over 9300 Å) is very poor and have not been used in any of the analysis.

3. Imaging

3.1. Morphology and surface photometry

Figure 1 shows the R band image obtained combining the different observations in this band (see also Fig. 1 of Kollatschny et al. 2000). The figure presents the grey-scale and isophotal maps in this filter. The high emission due to the activity of the galaxy NGC 7603 saturates the image in the central part of this galaxy. The system NGC 7603–NGC 7603B appears to be surrounded by a diffuse halo that we have been able to delineate out to 26.2 mag/arcsec^2 in the Sloan r-band filter. Although this halo seems to be associated mostly with NGC 7603, it is not symmetric with respect to this galaxy. There is evidences of a fainter extension tail in northern direction. The last isophote of the halo is also asymmetric to the West, possibly including a counter arm of the bright filament between NGC 7603 and NGC 7603B. The halo+filament between NGC 7603 and NGC 7603B shows up clearly and has a maximum brightness of 22.9 mag/arcsec^2 in the Sloan r-band filter, while the halo has a brightness near the filament of 23.4 mag/arcsec^2. Therefore, the filament alone has around 24.0 mag/arcsec^2. Another diffuse structure is seen apparently connecting NGC 7603 and NGC 7603B also, and situated to the South of the main filament. A point like object (#17 of Fig. 4) situated in the southest point of this tail has been also observed spectroscopically (see below) resulting a local star.

Fig. 2 shows a map of contours of the Hα emission in the IAC39 filter (centred on the redshift of the galaxy NGC 7603) once the continuum (R-filter) is roughly subtracted. No emission was found in the IAC35 filter (centred on the redshift of the galaxy NGC 7603B), either in NGC 7603B or in the filament. Only the nucleus of the NGC 7603 (IAC39 filter) shows some emission, as expected from a Seyfert 1 galaxy. No stripped emission regions (as found, for instance, in the stripping event in Stephan's quintet; Sulentic et al. 2001, Gutiérrez et al. 2002) were observed. This absence of Hα emission lines in NGC 7603B has already been pointed out by Sharp (1986). The non-detection of emission lines is not proof against the existence of a physical connection. In interactions and ejections with a larger galaxy, the gas is often stripped out of a stellar system (Rose et al. 2001); so

[5] IRAF is Image Reduction and Analysis Facility, written and supported by the IRAF programming group at the National Optical Astronomy Observatories (NOAO) in Tucson, Arizona.

the lack of emission lines could be taken as an indication of interaction rather than non interaction (pointed out by Sharp 1986).

Figs. 1, 2 and 3 show that NGC 7603 and its filament are apparently distorted by significant tidal interaction. The own existence of the filament is also a possible sign of tidal interaction or a debris from satellite disruption (Johnston et al. 2001). The fainter southern filament (the one which crosses object #17) and the red fringe embedded in NGC 7603 (red colour in Fig. 3; due possibly to dust) reinforces the scenario with tidal debris. The colour of the filament connecting NGC 7603 and NGC 7603B is an average one: $(g-r) \approx 0.95$ (equivalent to $(B-V) \approx 1.15$, like, for instance, in the bridge of the interacting system Arp 96; Schombert et al. 1990), $(u-g) \approx 1.5$, like the outer region of NGC 7603, and there are not emission lines in the filament (Paper I). The colour of this filament is relatively blue compared to the average value in the sample of tidal features by Schombert et al. (1990).

3.2. The Neighborhood of NGC 7603

First, we looked for QSOs, since they are typical objects among anomalous redshift candidates. We try to identify QSOs with $z < 2.5$ in the field using the multicolour criteria proposed in the analysis of the 2dF Survey (Boyle et al. 2000; Meyer et al. 2001). This criterion, converted into Sloan filters through the relations between the UBVRI Johnson filters and ugri Sloan filters given by Smith et al. (2002), and the relation between the photographic filter b_j and Johnson filters: b_j=B-0.28(B-V) (Meyer et al. 2001); (we adopt the approximation of U, R photographic-filters equivalent to U, R Johnson-filters) is:

$$(g-r) < \left\{ \begin{array}{ll} \frac{0.552-(u-g)}{0.381}, & (u-g) < 0.452 \\ \frac{0.921-(u-g)}{1.793}, & 0.452 < (u-g) < 1.197 \\ -0.154, & (u-g) > 1.197 \end{array} \right\}. \quad (1)$$

The completeness is quite high; this criterion covers $80-90\%$ of all QSOs (Meyer et al. 2001). The principal contamination comes from Galactic stars, subdwarfs and white dwarfs, and blue compact emission-line galaxies (Croom et al. 2001). The total fraction of the contaminant sources is $\approx 45\%$ (Croom et al. 2001). Therefore, the total number of QSOs will be $\approx 2/3$ times the number of objects that follow the criterion of eq. (1). This number is slightly different when the range of magnitudes is different from those of the 2dF survey, but not by too much.

We proceed as follows: first we select all objects in the field detected in the u filter. There are 38 objects in the u filter, including the two knots in the filament, but excluding NGC 7603 and NGC 7603B. We used the software "Sextractor" (Bertin & Arnouts 1996) to measure the photometry of these objects in u, g, r, i filters. For the two objects in the filament first we tried to subtract the contribution of the filament by a two-dimensional surface fit. Although we tried with different functions, ranges, etc., the result

was not perfect satisfactory partly owing to the presence of the two main galaxies, but the accuracy in the estimation of the magnitudes for these two objects is good enough within an uncertainty of $\sim$ 0.2 mag. Also, the photometry of object #35 was done separately because it was embedded in the halo of NGC 7603, taking special care of sky subtraction. It is noteworthy that object #35 has a quite high value of (g-r)=1.8, while (u-g)=0; although it does not follow eq. (1), it may be a unusual object because of its colours. Table 2 presents the results on the photometry in u, g, r and i of all the objects, whose positions are shown in Figure 4. We have no u magnitude for object #1 because it is too faint in this filter. Figure 5 presents a colour-colour diagram for these objects, and the regions in which QSOs are expected. We see that objects #19, #23 and #36 follow the criterion of eq. (1), which is indicated in Figure 5.

3.2.1. **Galaxies in/behind the filament**

We want to pay attention now to objects 1, 2, either embedded in the filament that joins NGC 7603 and NGC 7603B or behind the filament. The two objects appear point like in our deep image in the R band (see above). The field of the filament was observed in the F606W filter with the Hubble Space Telescope. It does not cover the other three narrow emission line galaxies, but we can examine how extended the objects are in the filament. Figure 6 shows this image. The field is centred on the filament between NGC 7603 and NGC 7603B and clearly shows the two objects within it. Both of them appear as extended objects; this is specially clear for object #1 (the one closer to NGC 7603). The figure also shows a contour plot of both objects which confirms the visual impression of both as extended objects. The FWHMs of objects 1 and 2 are $\sim$ 0.3 and $\sim$ 0.4 arcseconds respectively, which is rather small to be measured in a ground-based telescope with seeing of 1 arcsecond, and seems to indicate that they are extended rather point like objects.

The two **objects** in the filament are apparently a little deformed, although the significance is not too high (the two lowest isocontours in Fig. 6 are $\sim 2\sigma$ and $\sim 3.5\sigma$ respectively over the average flux in the region). The tail of object #1 in the northern part is warped pointing towards NGC 7603; and object #2 has some faint apparent tail in the northern part but this tail is less significant.

With the R band imaging we have studied the possible variability of these objects. In addition to the weakness of these objects, the presence of the filament makes the estimation of the magnitudes more difficult. In order to carry out the measurements, we first fit a two-dimensional surface to the filament excluding the region with the two objects. We estimate the uncertainties in the magnitude for these two objects as $\sim$ 0.2 mag. We have calibrated with standard stars only the R image taken on 2000 June 13, but we have performed differential photometry of the other images with eight bright

Table 2. Magnitudes of the objects in the field of NGC 7603 derived using "Sextractor" (except those marked with *, which were derived separately with "phot" taking care of the filament/halo subtraction and are affected by an error of at least 0.2 mag.). Last column points out whether they are extended "E" (as far as we can see from the available images and spectra; some furhter faint objects which look point-like might be extended too).

#	u	g	r	i	Ext.
1	—-	23.1(*)	21.7(*)	21.6(*)	E
2	23.8(*)	22.9(*)	22.2(*)	21.8(*)	E
3	20.7	19.4	18.7	18.6	E
4	20.9	18.1	16.6	16.0	
5	21.8	19.7	18.9	18.8	
6	18.6	17.3	16.7	16.7	
7	22.6	21.0	20.4	20.0	E
8	17.6	16.0	15.3	15.1	
9	22.9	21.1	20.5	20.2	E
10	21.5	21.2	20.4	20.5	
11	23.7	21.8	20.5	20.2	
12	23.3	22.4	21.3	21.2	
13	19.7	18.6	18.1	18.2	
14	23.1	21.2	20.5	20.4	E
15	21.2	20.1	19.6	19.6	
16	21.4	20.5	20.0	19.8	
17	20.6	20.0	19.4	19.5	
18	21.1	19.4	18.5	18.6	
19	22.5	22.4	22.0	21.6	
20	17.6	16.4	15.7	15.8	
21	21.9	20.5	19.5	19.2	E
22	22.0	21.4	19.9	19.7	E
23	21.6	21.6	20.8	20.6	E
24	19.4	17.9	17.0	17.0	
25	20.7	19.7	19.1	19.2	
26	22.4	19.3	17.8	17.2	
27	21.9	21.2	20.4	20.0	E
28	20.3	18.6	17.7	17.5	E
29	19.3	17.3	16.2	16.0	E
30	19.0	17.8	17.2	17.1	E
31	23.0	20.2	18.8	18.4	
32	21.3	20.2	19.6	19.3	E
33	23.4	22.0	20.8	20.1	E
34	23.8	22.3	21.0	20.1	E
35	22.8(*)	22.8(*)	21.0(*)	21.6(*)	
36	23.4	23.3	22.5	—-	
37	22.7	21.6	21.1	20.5	

stars in the field. According to the mentioned uncertainties, we conclude the absence of variability above $0.3 - 0.4$ mag.

4. Spectroscopy

The QSO candidates are in general too faint for spectroscopy with a 4.2 m telescope. In any case we used this telescope: 1) to corroborate and improve the spectra of both objects ($z = 0.24$ and $z = 0.39$) in the filament; 2) to obtain the redshift and classifications of some other objects in the halo of NGC 7603 (objects like #17, #21, #22 were interesting because of the peculiar position that they occupy with respect the halo and filaments of NGC7603; (Fig. 1 shows that these sources lie within the halo of NGC 7603); 3) to observe AGN candidates which are not too faint.

Table 3 summarizes the objects crossed by the three positions of the slit and a summary of the analysis of the spectra. Only the intense lines were used to determine the redshift. Figur 4 plots the positions of these slits. The spectra of the filament is poor because the slit in position 1 does not exactly crosses the maximum flux region of the filament, and the width of the slit (1.2 arcsec) is small compared with the slitwidth of 5 arcsec used in the observations taken with the NOT and presented in Paper I ([OIII] detections reported in Fig. 2b of Paper I were spurious). The **main spectral features** of these objects **corrected of redshift** and the new ones (objects #21, #22, #23) are shown in Figure 7. All of them are narrow emission line galaxies.

Table 4 gives the values of the equivalent widths of the different lines. Apart from the errors pointed in the table due to noise in the spectra, these equivalent widths are subject to the possible errors in the subtraction of the sky emission(+filament in objects #1, #2). Although the absolute values of EWs can only be taken as a rough approximation, the ratio of close lines is rather exact (because here the uncertainties in the continuum cancel). Roughly, the error would be a factor ~ 2 for the continuum in the worst of the cases (assuming the error in the subtraction of the sky+filament is equal to its Poissonian noise), which means that in the worst of the cases the error of EW is a factor two too.

The spectral classification of narrow emission line galaxies is usually made through the flux ratios of specific lines corrected of reddening, assuming a constant intrinsic ratio for $\frac{F_{\rm intr.}(H\alpha)}{F_{\rm intr.}(H\beta)}$. However, this ratio changes when the physical situation in the galaxies does not obey a simple model moreover, we have extinction from the dust in the own galaxy plus the extinction of the filament in cases of #1 and #2, and some minor contribution from the Galactic extinction, which are difficult to separate. In order to classify the galaxies, we use the ratios of lines that are close in wavelength. The difference between the flux ratio and the equivalent width ratio is neglected. The spectral classification criteria is based on the ratios $\log \frac{\rm OIII_{5007}}{\rm H\beta}$ and $\log \frac{\rm NII_{6584}}{\rm H\alpha}$ (given in Table 4) (Veillux & Osterbrock 1987, Filippenko & Terlevich 1992, Dessauges-Zavadsky et al. 2000), and gives the result

Table 3. Spectral analysis. The error in the redshift is $\approx \pm 0.002$. The codes for the last two columns are: 0-absorption emission line galaxy; 1-narrow emission line galaxy; 2-star; 3-contamination by the filament; 4-spectra very noisy.

Slit pos.	Object	Spectral features ($> 3\sigma$)	Redshift	Type	Notes
1,3	NGC 7603B	CaH&K, MgI, NaI, etc.	0.056	0	
1	#1	OII, Hβ, OIII, OI, Hα	0.394	1	
1	#2	OII, NeIII, Hβ, OIII, Hα	0.245	1	
1	Filament	Hβ, MgI, NaI	0.030	Abs.	4, Paper I
2	#17	Hα, Hβ	0	2	3
2	3.6"-WNW of #17	—-	—	—	4
2	#19	—-	—	—	4
2,3	#21	$OIII_{5007}$, Hα, NII, SII	0.117	1	
2,3	#22	OII, Hβ, Hα	0.401	1	
3	#23	Hα	0.246	1	

that the objects in table 4 are HII-galaxies except object #21, which might be either a HII-galaxy or a LINER (since its continuum is strong and the emission lines are faint, it might be a "Low Luminosity Active Galactic Nuclei"; Maoz et al. 1998).

Table 4. Equivalent widths (in angstroms) of the emission lines of the five observed narrow emission line galaxies. Errors include a rough determination of the noise and the error in the determination of the continuum, but do not include the error in the subtraction of the sky(+filament in objects #1, #2).

Line	Object #1	Object #2	Object #21	Object #22	Object #23
OII_{3727}	56.3±6.1	36.2±7.3	37.1±9.3	15.3±2.1	68.4±75.1
$NeIII_{3869}$		13.0±3.1			
Hβ	13.5±1.1	43.3±4.5	3.3±0.8	6.9±1.1	3.7±1.5
$OIII_{4959}$	11.2±1.2	62.8±6.3			
$OIII_{5007}$	19.2±1.7	172.3±22.1	2.6±0.5	2.3±0.9	3.5±1.5
OI_{6300}	11.7±2.4			17.0±6.1	
Hα+NII_{6548}	81.0±21.9	160.9±26.2	15.6±0.7	25.9±5.4	18.5± 4.3
NII_{6584}	16.2±7.3	8.8±4.6	8.4±0.5	6.2± 3.1	1.8±1.8
$SII_{6717+6731}$			7.3± 0.7		
$\log \frac{OIII_{5007}}{H\beta}$	0.15±0.05	0.60±0.07	-0.10±0.13	-0.48±0.18	-0.02±0.26
$\log \frac{NII_{6584}}{H\alpha}$	-0.70±0.23	-1.26±0.24	-0.27±0.03	-0.62±0.24	-1.01±0.45

4.1. Galaxies in/behind the filament

The HII-galaxies embedded in the filament, #1 and #2, seem to be indeed a quite peculiar star-forming galaxies. The very intensive $H\alpha$ (equivalent width: EW(Hα) $\approx$ 80 Å and 160 Å resp.), if correct (i.e. if the continuum is really as low as obtained by us and the sky+filament subtraction has not changed the level of the continuum; roughly, error of EW should be a factor two at most), would be indicative from a vigorously star-formation galaxy. Only $\sim 2\%$ and ~ 1 % resp. of the normal HII-galaxies have a so high EW(Hα) (Carter et al. 2001). However, if they were dwarf HII-galaxies, these high EWs would be within the normal expected values. The mean intrinsic colour of these objects is $(B-V)_0$=0.22 mag and $(B-V)_0 = 0.10 \pm 0.2$ resp. (with a dispersion of ≈ 0.10 mag, plus an error of ~ 0.15 mag due to the factor 2-error in the value of EW; total: $\sim \pm 0.2$ mag) (Kennicutt et al. 1994, Fig. 2a).

We apply the correction of extinction for the flux of these objects in the following way. First, we derive the observed $(B-V)_0$ in the reference system of the galaxy [i.e. we calculate the equivalent (B-V) in the redshifted wavelengths; we do this through the calculation of the flux in the corresponding wavelengths of the redshifted B and V filters given the UBVRI fluxes; this is equivalent to make the k-correction]. These are: $(B-V)_0 = 0.58$ (object #1) and $(B-V)_0 = 0.45$ (object #2). We neglect the difference between the colours of a face-on galaxy and other inclinations. Therefore, the differences between these measured colours and the colours expected for these HII-galaxies with the corresponding $EW(H\alpha + [NII])$ are: $\Delta(B-V)_0 = 0.48 \pm 0.2$ (object #1) and $\Delta(B-V)_0 = 0.23 \pm 0.2$ (object #2). We assume that the measure of the colour has negligible error (the absolute magnitude in each filter has 0.2 mag. of error, due to the contamination of the filament, but in the measure of the colour, since the technique to decontaminate from the filament is the same, this error cancels). We attribute these differences to the extinction produced by the filament ($z_{\rm fil} = 0.030$) plus the Galactic extinction ($z = 0$):

$$\Delta(B-V)_0 = A_{\rm Gal.}[\lambda_B(1+z)] - A_{\rm Gal.}[\lambda_V(1+z)]$$
$$+ A_{\rm fil.}\left[\lambda_B \frac{(1+z)}{(1+z_{\rm fil})}\right] - A_{\rm fil.}\left[\lambda_V \frac{(1+z)}{(1+z_{\rm fil})}\right]. \quad (2)$$

The Galactic reddening is relatively low: $[A_{\rm Gal.}[\lambda_B(1+z)] - A_{\rm Gal.}[\lambda_V(1+z)] = 0.03$ for both objects according to Schlegel et al. (1998) maps of extinction. Assuming a reddening due to the filament similar to the Galactic dust [$A(\lambda)/A_V$ from Mathis 1990], we get

$$A_{\rm fil.(obj.\ \#1)}[\lambda' = \lambda/(1+z_{\rm fil})] = (2.0 \pm 0.9)\frac{A(\lambda')}{A(\lambda'_V)}, \quad (3)$$

and

$$A_{\rm fil.(obj.\ \#2)}[\lambda' = \lambda/(1+z_{\rm fil})] = (0.9 \pm 0.9)\frac{A(\lambda')}{A(\lambda'_V)}, \quad (4)$$

The corrected magnitudes, including Galactic and filament extinction correction, are written in Table **??**.

The calculation of the absolute magnitudes, for instance for the filter V [in the own galaxy, i.e. $\lambda = \lambda_V(1+z)$], can be carried out by means of:

$$M_V = m_{\rm corr.ext.}[\lambda_V(1+z)] - 5\log(D_{\rm Mpc}) - 25, \quad (5)$$

$$D_{\rm Mpc} = \frac{c(1+z)}{H_0}$$

$$\times \int_0^z [(1+x)^2(1+\Omega_M x) - x(2+x)\Omega_\Lambda]^{-1/2} dx. \quad (6)$$

We assume $H_0 = 71$ km/s/Mpc, $\Omega_M = 0.27$, $\Omega_\Lambda = 0.73$ (derived from WMAP data; Bennett et al. 2003). If we consider the redshifts as indicator of the cosmological distance: $M_V(object\#1) = -21.5 \pm 0.8$, $M_V(object\#2) = -18.9 \pm 0.8$. If we considered an anomalous intrinsic redshift case (in such a case, in order to derive the distance, we set $z = z_{\rm fil} = 0.03$), the results are: $M_V(object\#1) = -15.2 \pm 0.8$, $M_V(object\#2) = -13.9 \pm 0.8$. In this second case, they would be in the faint tail of the HII-galaxies, type II (Telles & Terlevich 1995); they would be dwarf galaxies, "tidal dwarfs" as in Stephan's Quintet (Lisenfeld 2002) but with anomalous redshifts, and this would explain the observed strong star formation ratio: objects with low luminosity have higher EW(Hα) (Carter et al. 2001). Teplitz et al. (2003) show examples of compact emission line galaxies with very high EW(Hα) and absolute filterless magnitudes between -14 and -15 (e. g., SPS J082344.12+292351.3).

4.1.1. Comparison with Paper I and corrections

With these new spectra, we confirm the redshifts of objects #1 and #2 observed in Paper I, and furthermore we detect the Hα emission line in the spectra of both objects. Now it is possible a more accurate estimation of the linewidth of each object.

In Paper I, the tenptative possible classification of both objects as QSOs (indeed, in Paper I we claimed that they were compact emission line objects, either QSOs or HII-galaxies) is not confirmed here. In Paper I, we had not analysed HST data so we could not see whether the objects had any extension. In Fig. 3 of Paper I, we pointed out that the $H\beta$ line in object #2 had a FWHM of 49 Å while the forbidden lines had 30 Å in these low resolution spectra; and the same thing was observed for object #1 with poorer signal/noise. However, in the present WHT-telescope higher resolution spectra, we have not observed this relative broadening, so we must think that the apparent excess broadening of Hβ in Paper I was an artefact due to noise.

In Paper I, we made a rought measurement of the parameter R_{23} directly from ratios of equivalent widths[6]; however, lines fluxes corrected for reddening would be necessary. The results presented in this paper by making use of EWs of close lines give in any case the same conclusion: they are HII galaxies (provided that they have narrow lines).

The slight differences in the R-magnitude (0.2 and 0.1 mag respectively) with respect to the values presented in Paper I are caused by differences in which the filament was subtracted and are within the error. In Paper I, it was claimed that the objects have $m_{b_j} < 21.9$ (corrected of extinction), and this is correct, but for a reason different from the arguments given in Paper I. They are intrinsically blue, but because of the extinction they are observed as red [$(B-V)_0 = 0.10$ and 0.22 respectively for objects #1 and #2 corrected for extinction and the k-correction] instead of blue as claimed in Paper I.

Summing up, we confirm the main results of Paper I, except in the tenptative statements such as the possible classification of objects #1 and #2 as QSOs.

5. Analysis

5.1. A candidate perturber

According to the results in §3.1, some close and not very faint neighbour must be in the surroundings of NGC 7603. If we assumed that NGC 7603B and NGC 7603 have the same distance, this filament would be clearly due to the interaction among both. Are there other possible candidates?

There is a galaxy with similar redshift, one magnitude fainter, and 10.3 arcminutes from NGC 7603: NGC 7589; or B231533.01-000313.1, three magnitudes fainter and 12.6 arcminutes of distance. However, both of them are in the opposite direction of the filament (in the west instead of the east). We do not find any other appropriate candidate for the interaction in the surrounding 30 arcminutes. Nonetheless, we cannot be sure that this companion object does not exist until we make the spectroscopy of all the surrounding objects around NGC 7603. For instance, galaxy #29 (see Fig. 4 and table 2) is four magnitudes fainter than NGC 7603 in B-filter, it has an angular distance of 2.5 arcminutes (linear distance larger than 100 kpc) and it seems to be in the direction of the tail which is extended towards north; it might be a candidate of companion to produce the tidal disturbances. Or galaxies #28, #30. Johnston et al. (2001) in their eq. (11)/Fig. 6 calculate the expected surface brightness magnitude in such cases. Assuming $t > 1$ Gyr a mass-to-light ratio of 10, rotation velocity from NGC 7603 of 200 km/s in the outer disc, and a distance of the satellite of 100 kpc we would have that the observed surface brightness in R of the filament should be > 27 mag/arcsec^2; however we observe

[6] There was also an erratum in the reference to Filippenko & Terlevich (1992) in Paper I: they said that LINERs have $\log_{10} \frac{OIII_{5007}}{H\beta} \leq 0.5$ instead of $\frac{OIII_{5007}}{H\beta} > 0.5$, and this is used to separate Seyfert 2s and LINERS rather than HII-galaxies from LINERs.

that it is 24 mag/arcsec^2. Therefore, it seems in principle not too probable, but it might be, and this remains as a possible solution within a standard cosmological redshift hypothesis scenario until it can be discarded with new spectroscopical observations of all the surrounding objects and/or calculations which proof that these faint objects cannot produce the observed tidal disturbances.

5.2. Statistics

In this section, we will carry out some statistical calculations in order to show how anomalous is the observed configurations: 1) to have up to two QSOs in the neighbourhood of NGC 7603; 2) to have the observed configuration of 4 objects with different redshift connected by a filament.

5.2.1. QSOs statistics

In §3.2, we concluded that there are three objects that follow eq. (1) within a radius $R = 1.5$ arcminutes from the center of NGC 7603 (the distance to object #36). One of these (object #23) is not a QSO (see §4). The other two were too faint to be observed spectroscopically with the available telescope and time (perhaps a larger telescope would be needed). Therefore, we have at most two QSOs in the field of NGC 7603 [indeed, some extra QSOs are possible, but with a low probability because the multicolour criterion covers 80-90% of all QSOs (see §3.2)] with $m_{b_j} = 22.6, 23.6$ (respectively for objects #19 and #36; derived from Sloan filters information as in §4.1).

The probability for such a event is (assuming roughly that p_i, the probability for the detection of each QSO, follows $e^{p_i} \sim 1$):

$$P_Q \geq \frac{(\pi R^2)^2 N_{\rm QSO}(m_{b_j} < 22.6) N_{\rm QSO}(m_{b_j} < 23.6)}{2!}. \quad (7)$$

According to the QSO counts from eq. (A.3), the probability is $P_Q \geq 0.029$, so one might expect these number of background QSOs to occur by chance (2.2-σ at most, if both candidates are confirmed as QSOs).

5.2.2. Probability of NGC 7603 and its 3 companions being a chance projection effect

From Figs. 1 of Paper I; and Fig. 4 or 6 of this paper, it seems extremely improbable that four objects at different distances can show a chance projection in the way these figures reveal. Statistics have been calculated in several ways for some time concerning the anomalous redshift problem (e.g., Arp 1981, 1999*a*; Burbidge et al. 1997), in order to assess the probabilities of peculiar configurations. However, many other authors (e.g., Noerdlinger 1975; Sluse et al. 2003) have suspected that many of these calculations are

unappropriate. Some authors also say that one should not carry out a calculation of the probability ("a posteriori probability") for an a priori known configuration of objects (for instance, that they are aligned, or that they form a certain geometrical figure) because all possible configurations are peculiar and unique. For example, if the Orion constellation is observed and we want to calculate the probability of their stars to be projected in that exact configuration, we will find that the probability is nil (it trends to zero as the allowed error in the positions of the stars with respect the given configuration goes to zero), but the calculation of this probability is worthless because we have selected a particular configuration which has been observed a priori. Therefore, the statistics to be carried out should not concern the geometrical figure drawn by the sources, unless that geometrical configuration be representative of a physical process in an alternative theory (for instance, aligned sources could be representative of the ejection of sources by a parent source). In this last sense, we think that many of the statistics already published are worthwile and indicate the reality of some statistical anomaly. The real question is to look for peculiarities associated with peculiar physical representations, not just peculiarities in the sense of being unique.

For our case, we will use a simple fact: the connection of four objects throughout a filament. This aspect represents a physical peculiarity, not because of their uniqueness but because they could be better represented by an alternative theory claiming that the four galaxies are at the same distance, three of them ejected with the filament by the parent galaxy NGC 7603. We are not going to determine the probabilities of forming triangles or any shape observed a priori. The peculiarity that we want to analyse is not comparable with the previous example of Orion because we have in mind a physical representation rather than the given peculiar distribution of sources. The difference from the Orion problem is that the peculiarity of Orion is not associated with any particular physical representation to be explained by an alternative theory. The question is as follows: what is the probability, P, of the apparent fact arising from a random projection of sources with different distances? Or, in other words, what is the probability, P, that the standard theory can explain the observed facts without aiming alternative scenarios? This probability is as follows: NGC 7603 has a filament of area A. The probability of having three further independent sources, with the corresponding magnitudes of the objects 1-3, projected on that filament is (assuming that the individual probabilities for each event p_i follow $e^{p_i} \approx 1$):

$$P_{=} \frac{A^3 N_1(m \leq m_1) N_2(m \leq m_2) N_3(m \leq m_3)}{3!}, \quad (8)$$

where N_i is the source density on the sky for the type of sources of object i with apparent magnitude less than m_i (magnitudes corrected for Galactic+filament extinction, in order to be comparable with the galaxy counts from appendix A), for the filter in which we know the magnitude of the source. We will use, for instance, filter B, but the statistics

would give similar results for any filter. Some authors (e.g., Sluse et al. 2003, hypotheses H2-H3) use in the calculation of the probabilities the limiting magnitude of the survey instead of the magnitude of the object, which gives a higher probability. However, this is not totally correct because, randomly, one would expect most of the detected objects to be close to the limiting magnitude. If this method is followed, the magnitude of the object and the limiting magnitude of the survey are very close and there are no major differences in the calculation; but, in the case the magnitude of the object being much brighter than the limiting magnitude one should multiply P by a factor that characterizes the probability this object being much brighter than the limiting magnitude (the brighter it is, the lower the probability), and this is equivalent to use the magnitude of the object. So we think that Sluse et al. (2003) hypotheses H2-H3 are inappropriate.

The area of the filament is approximately 35 arcsec in length multiplied by 4 arcsec in width (the area plotted in Fig. 6):

$$A \approx 35\text{”} \times 4\text{”} = 140 \text{ arcsec}^2 = 1.1 \times 10^{-5} \text{ deg}^2. \quad (9)$$

We are not going to use other peculiarities of the system like the fact that objects #1 and #2 are positioned where the filament contacts NGC 7603B and NGC 7603 respectively. Neither, are we going to use the fact that two of the three galaxies are HII-galaxies; we pay no attention to galaxy type. Neither, are we going to use the distribution of redshifts (from major to minor). If we took these facts into accounts, the probability P would be somewhat lower.

NGC 7603B is a galaxy with $m_{B,1} = 16.6$ (Sharp 1986, corrected only for Galactic extinction; it would be less if the foreground filament produced any extinction in the galaxy). And the magnitudes corrected for extinction of the two HII-galaxies are: $m_{B,2} = 21.1 \pm 1.1$ and $m_{B,3} = 22.1 \pm 1.1$. With all these numbers, and the counts given by eq. (A.2), the deduced probability is

$$\log P = -8.6 \pm 0.8. \quad (10)$$

The error is large, due to the uncertainty of 1.2 mag in the objects #1 and #2, but the order of magnitude does not change too much. This means that we have a probability of a few times 10^{-9} of finding three galaxies of any type by chance with different distances projected on a filament (an arm or another structure) with an area of 140 arcsecond^2 of an arbitrary galaxy with respective apparent magnitude (corrected for extinction) less than or equal 16.6, 21.1, 22.1 respectively, and somewhat higher if the magnitudes are up to 1.2 fainter in the last two objects. If there were no filament extinction at all, the value of $\log P$ would be -7.1. There are certain facts that could make the probabilities calculated above larger. For instance, the density of any of the objects would be significantly larger than we have assumed, if the distribution of any of these sources were clustered in some specific regions, or if there were bias selection effects. There is not justification for a conspiracy in

which our line of sight crosses three clusters of galaxies at different redshifts ($z = 0.056$, $z = 0.245$ and $z = 0.394$). However, maybe at least one of the objects is in a cluster (for instance the object at $z = 0.245$ since we have found another object with $z = 0.246$ not very far away). In any case, the increase in the probability due to the increase of the density in lines of sight with clusters is compensated with the additional factor to be multiplied by the present amount P to take into account the probability of finding clusters in the line of sight. On average, in all the arbitrary lines of sight on the sky, the probability will be given anyway by the above value of P (see further discussion in §5.3.1). With regard bias selection effects, there are no such biases, because we have used complete galaxy counts from complete surveys up to a given magnitude (appendix A).

Furthermore, we could multiply P by the probability to have two extremely vigorous star formation in the HII-galaxies, P_2. The calculation of P_2 (with probabilities $\sim 1\%$ and $\sim 2\%$ for each galaxy, as said in §4) is

$$P_2 = 0.01 \times 0.02 = 2 \times 10^{-4} \tag{11}$$

There is nearly independence between both probabilities, so the global probability is the product of P and P_2. There is a correlation between absolute magnitudes and the star formation ratio: the fainter the HII-galaxy, the higher is the star formation ratio (Carter et al. 2001). As a matter of fact, Teplitz et al. (2003) find in their sample that many galaxies have large values of EW(Hα) but their objects are in general intrinsically fainter. However, as has already been said, if we accept the cosmological redshift hypothesis, our two HII-galaxies would have average or high luminosities (absolute magnitudes in V from -19 to -22); therefore, it is not possible and enhancement of the probability due to some selection effect (neither Malmquist bias nor the opposite one). In any case, we will not consider the low value of P_2 until we can have more accurate measures of EWs, and we will only discuss the probability P quoted above.

We have found this extraneous combination of circumstances (if we adopt the hypothesis of cosmological redshifts) by accident. We did not sistematically analyze all the Seyfert galaxies like NGC 7603 in order to find something like this. Even if we have made a complete analysis of these characteristics, to observe only one object with a probability 3×10^{-9} would still be very small. According to SIMBAD there are 237 AGN-galaxies in all the sky with a B magnitude less than 14.0 (the magnitude of NGC 7603; de Vaucouleurs et al. 1991). Therefore, the probability to have an AGN with a B magnitude up to 14.0 with a cluster of coincidences that we observe in NGC 7603 is:

$$P_{\text{all AGNs,m}_\text{B}<14.0} \sim 7 \times 10^{-7}. \tag{12}$$

Some alternative theories (Arp & Russell 2001, Burbidge 1999b) do predict that Seyferts eject galaxies so the statistics with AGN makes sense. However, even if we decided to use all the galaxies, independently of whether they are AGNs or not, according to SIMBAD

the number of galaxies with $m_B < 14.0$ is 3655, so the probability of finding a galaxy with a B magnitude up to 14.0 with the cluster of coincidences that we observe in NGC 7603 is:

$$P_{\rm all\ galaxies, m_B<14.0} \sim 10^{-5}, \quad (13)$$

This assumes that all the galaxies have some filament/arm like NGC7603 to find the background objects, which is not necessarily the case, so we are overestimating the probabilities. And these probabilities are calculated assuming that there is only one case with this cluster of chance circumstances. This could not be the case because not all the systems have been studied in detail, and some of the cases which were studied with some detail also present similar coincidences. For instance, cases like 3C212 (Stockton & Ridgway 1998), NGC 3067 (Carilli et al. 1989; Carilli & van Gorkom 1992), NGC 3628 (Arp et al. 2002); NGC 1232, NGC 4151 or NGC 622 (Arp 1987); or the cases mentioned in Arp (1980) also present some filaments/arms that have at their ends, or somewhat beyond the end in the direction of the filament, some galaxy or QSO with different redshift (Note: many of these examples have however magnitude large than 14.0 in B). Another possible example might be the tail between NGC 7320 and NGC 7318 in Stephan's Quintet (Moles et al. 1998; Gutiérrez et al. 2002; Williams et al. 2002). In some of these tails the presence of dwarf galaxies looking like objects 1 and 2 has been discovered even at relatively large distances from the disrupted galaxy (Gallagher et al. 2001). So, again, we are overestimating the probability because we are only considering one case among all galaxies, and there are other coincidences too.

It is remarkable that the presence of the filament gives the configuration a low probability, but even without taking into account the presence of the filament, the probability is still somewhat low too. Given a square of diagonal 59 arcseconds (the separation between NGC 7603 and NGC 7603B), the chance to have there four galaxies with magnitudes in the B-filter of 13.8 (the magnitude of NGC 7603 corrected for extinction), 16.6, 21.1 and 22.1 would be 3.5×10^{-11} [again with Poissonian statistics and the counts given by eq. (A.3)]. There are 3.2×10^8 squares like this on the whole sky, so the probability of finding only one square in the whole sky with this congregation of four objects of different distances is 1.1×10^{-2}. A 1% probability is not extremely low, but taking into account that this is the probability for the whole sky, and that it would have average properties, this low number is also somewhat strange.

Summing up, even in the worst of the cases, we have that the probability to find only one case like the present three background galaxies of the given magnitudes in the filament/arm among all galaxies up to magnitude 14.0 in B-filter is around 10^{-5}, so we consider that it is justified to talk about "anomaly". The question now is to find the reason for this low probability and whether it can be explained in terms of a cosmological redshift or not.

5.3. Possible explanations for the low probability observed configuration

Possible scenarios to explain the present case of NGC 7603 depend on the possible explanations for the redshift of the objects are (Narlikar 1989; Hoyle & Burbidge 1996): cosmological (with the observed configuration due to clusters in the line of sight, or gravitational lensing), Doppler, gravitational or others. In this section, we are going to discuss how well the different hypotheses explain the present case.

5.3.1. Clusters in the line of sight?

Perhaps we have found a line of sight with many clusters of galaxies, that increases significantly the density of sources with respect to a Poissonian distribution. However, as explained in §5.2.2, a conspiracy in which our line of sight crosses three clusters of galaxies at different redshifts ($z = 0.056$, $z = 0.245$ and $z = 0.394$) is not justified because the increase in the probability due to the increase of the density in lines of sight with clusters is compensated with the additional factor to be multiplied by the present amount P to take into account the probability of finding clusters in the line of sight. In average, in all the arbitrary lines of sight of the sky, the probability will anyway be given by the above value of P. We can illustrate this argument with some simplistic calculations. Let assume that the clusters in the sky have the same size, A_c, a Poissonian distribution, and the same number of galaxies up to a given magnitude, n_c (galaxies/cluster). This is a very rough model, because it is clear that A_c and n_c depend on the redshift; however, for our present arguments, the estimation with mean values of A_c and n_c is enough. In such a case, the total counts of galaxies, N, is:

$$N = N_f + N_c n_c, \tag{14}$$

where N_f is the density of field galaxies (galaxies/deg^2) and N_c is the density of clusters (clusters/deg^2). An example of a probability calculation would be the one to have three galaxies belonging to three different clusters in the area A (we assume that they have the same magnitude, for a simplistic calculation, although it can be generalized to any magnitude distribution), i.e. the probability three clusters being in the line of sight multiplied by the probability of three galaxies from different clusters being in the area A of the filament given the density of galaxies in a cluster,

$$P = \frac{(N_c A_c)^3}{3!} \frac{\left(A\frac{n_c}{A_c}\right)^3}{3!}$$
$$= \frac{A^3 N^3}{3!}\left(1 - \frac{N_f}{N}\right)^3 \frac{1}{3!} < \frac{A^3 N^3}{3!}, \tag{15}$$

that is, the probability is lower than $\frac{A^3 N^3}{3!}$, which is the probability we calculated in (8). Therefore, the supposition of a line of sight with three clusters in the line of sight

would make the probability smaller instead of larger, and similarly for a lower number of clusters.

Indeed, it is not likely to find clusters of galaxies at $z = 0.245$ and $z = 0.391$, in spite of the two pairs of HII-galaxies with close redshifts, because HII-galaxies are much less common in clusters than in field galaxies (Gisler 1978; Dressler et al. 1985; Biviano et al. 1997), i.e. the probability of finding HII-galaxies in clusters is much lower than among field galaxies. Therefore, unless we want to introduce a new factor that further reduces the value of P (which makes the problem more difficult to solve in terms of cosmological redshift rather than solving it), we must not see the solution of the clusters as a way to explain the problem in normal terms of probability .

Nonetheless, although the low probabilities cannot be justified by this scenario of clusters, and although the high star formation ratios seem to point in the opposite direction, we also have object #23 with nearly the same redshift as object #2, and object #22 with a difference of 0.007 in redshift with respect to object #1. They are not necessarily in the same cluster, but perhaps they form small groups of galaxies with separations of 0.5 or 2 Mpc (for the pairs at $z = 0.25$ and $z = 0.40$ respectively). Therefore, this standard scenario, even though it cannot explain the statistical problem, should be still borne in mind. We have considered above that the distribution of clusters is Poissonian; it might be that we have detected two or three clusters in the line of sight for some special reason. Could our line of sight be tangential to a wall or sheet within the large scale structure, for instance? This seems difficult to imagine, since we would need a wall of size 2 Gpc. The Hydro-Gravitational Theory (Gibson 1996; Gibson & Schild 2003) would claim that the members of a cluster (NGC 7603, NGC 7603B, object #1 and object #2) formed together, and that they remained together until the uniform expansion of space in the universe finally overcame the gravitational and frictional forces of the cluster, and the different galaxies separated with very small transverse velocity with respect the line of sight because of the halo gas friction and their sticky beginning. The stretching would be along a pencil beam of length ~ 2 Gpc in the line of sight by the expansion of the universe, but a preferred direction of the expansion instead of an isotropic expansion it is not justified; why the expansion along the line of sight is not sticky as it is for the other directions? These are in any case speculative possibilities which are not compatible with the CDM theory of the formation of the large scale structure. The question, therefore, remains open.

5.3.2. Gravitational lensing

A better explanation might in principle be found if we considered some kind of gravitational lensing. For instance, amplifications up to a factor ~ 30 are expected (Ellis et al. 2001) for background objects apparently close to the central parts of massive clusters.

The effect produced by an individual galaxy like NGC 7603 should be much smaller, and the low redshift galaxy ($z = 0.029$) NGC 7603, as the putative lens of very distant sources ($z = 0.245$ and $z = 0.394$) would have a very small amplification because of the large angular distance of the sources. Some rough calculations can illustrate this argument; given a galaxy with Einstein radius θ_E, the enhancement in the density of background objects as a function to the angular distance, θ, to this galaxy will be (Wu 1996):

$$q_Q(\theta) = \frac{N[m < m_{b,lim} + 2.5 \log \mu(\theta)]}{N(m < m_{b,lim})} \frac{1}{\mu(\theta)}, \tag{16}$$

where μ is the magnification factor (Wu 1996),

$$\mu(\theta) \approx \frac{\theta}{\theta - \theta_E}. \tag{17}$$

In order to have a value of P that is not very low, we would need this to be $\sim 10^3 - 10^6$ higher, i.e. an average enhancement of $\sim 10-100$ in density for each of the galaxies. With the counts of eq. (A.2), for the lowest enhancement, this requires an average magnification of $\mu(\theta)$ of $\sim 2 \times 10^4$. We would need to be in the ring $\theta_E < \theta < \theta_E(1 + 5 \times 10^{-5})$, which is very narrow with a very low probability; so again the problem is not solved by this artefact. It is clear from eq. (16) that the density of sources does not increase so quickly, unless the counts increase extremely quickly with the limiting magnitude, which is not our case. This is so because the enhancement in the source counts increases because of the flux increase of each source but decreases because of the area distortion, which reduces the number counts by losing the sources within a given area (Wu 1996).

In our case, since the distance of the sources to the centre of NGC 7603 is 0.5-1 arcminute, we would need either a very large value of the Einstein radius of the gravitational lens placed in the centre of NGC 7603, which would require a huge mass (for instance, an average E/S0 galaxy has a $\theta_E \approx 1.33$ arcseconds, Wu 1996), or that the gravitational lenses be not so massive but much closer to the magnified objects. The first possibility may be automatically rejected, since even in the case that NGC 7603 had the mass of a cluster of galaxies, the magnification would affect at most only one of the three objects in the filament, the one closer to its Einstein radius. The second hypothesis, the possibility that multiple minilenses are distributed in the halo of the galaxy, has already been proposed: gravitational mesolensing by King objects (Baryshev & Bukhmastova 1997; Bukhmastova 2003). The strong gravitational lensing would be produced by King lenses: globular clusters (Bukhmastova 2003), dwarf galaxies, or clusters of hidden mass with masses between 10^3 and 10^9 $M_\odot$. This is an interesting idea, although we are not convinced by the proof presented by one of authors of the idea (Bukhmastova 2001) which reveals excesses of pairs of galaxy/QSO with $z_{gal} > 0.9 z_{QSO}$, because many of these pairs were indeed the same object classified both as QSOs and galaxies. Anyway, the idea is interesting, and it might be considered as a serious proposal for solving the statistical correlations between QSOs and galaxies in large surveys. Nevertheless, in our

particular case, it does not solve the low probability P, because, as has been said, only in narrow rings is the enhancement high enough, and these narrow rings have a very small area, so, again, the probability of these being a large number of sources is small.

5.3.3. Non-cosmological redshift hypotheses

The relative angular configuration of NGC 7603, NGC 7603B, object #1 and #2, the filament connecting all of them (and, the probability that two of two HII-galaxies in the filament have very high star formation ratios, if we accepted as valid the measures of the EWs) would be naturally explained as a consequence of a physical interaction between them. An interpretation which explains the configuration as equivalent to other systems in interaction would be clearly preferred over one in which the configuration is purely a projection effect according to the calculations in §5.2.2. In that case, the filament would be a sign of disruption in NGC 7603 owing to the proximity of NGC 7603B. This is reinforced by the fact that both NGC 7603 and NGC 7603B show asymmetries in the halo. The narrow emission line galaxies #21, #22, #23 in the other side of NGC 7603 might also be embedded into the extension of the halo pointing to these objects.

In such a case, the redshifts would be non cosmological. Some of the possible explanations for an intrinsic redshift with standard physics are now discussed:

Doppler: Considering only the system of NGC 7603 and NGC 7603B, which have a difference of around 8000 km/s is it possible that both galaxies are at the same cosmological distance and that the difference in redshift reflects a difference in peculiar velocities? The known examples of interacting galaxies in the field show differences in velocity between to ~ 1000 km s^{-1}. The larger density of objects in a cluster of galaxies and the dispersion of velocities within them could favour high speed collisions with differences in velocity between the interacting galaxies of a few ~ 1000 km s^{-1}. The possibility of an encounter between groups of galaxies with a difference in velocity of ~ 4000 km·s^{-1} has been considered by de Ruiter et al. (1998) as a possible explanation of the peculiar field around B2 1637+29. However, as far as we know, no example of such a collision in the field with a difference in velocity as large as that existing between NGC 7603 and NGC 7603B has been reported so far, and it would be unexplained in the framework of models of galaxy formation. Furthermore, the extremely high velocity differences of the HII-galaxies would disrupt the system quickly and there would be cases of blueshifts (in this or other anomalous redshift cases).

Gravitational: Anomalous redshifts could alternatively be explained in terms of highly collapsed matter (Narlikar 1989). The gravitational redshift explanation could then be an explanation in terms of standard physics although we would need either very high masses or very low radii for these objects. High mass seems to be excluded since this

would affect the rotation curves in the QSO-galaxy pairs (Hoyle & Burbidge 1996). Very dense non-high mass objects could explain the situation, but the HII-galaxies and NGC 7603B are extended objects; unless most of the mass is concentrated in the very centre of the nucleus, giving an intrinsic redshift, and the outer part of the galaxies had normal cosmological redshifts. At present, we have not detected these differences of redshifts within the HII-galaxies, and it can surely discarded for NGC 7603B.

Multiple scattering: Dynamic multiple scattering has been also proposed to explain these systems. Results in statistical optics (Wolf 1986; Datta, Roy & Moles 1998a, b) show that a shift in the frequency of spectral lines is produced with redshift independent of the frequency when the light passes through a turbulent (or inhomogeneous) medium, because of multiple scattering effects (Roy et al. 2000). Perhaps, the anomalies could be caused by certain special conditions in the surroundings of the anomalous redshift objects. Indeed, the scattering solution was proposed a long time ago as a way to explain the loss of energy of the photons ("the tired light theory"), an alternative to the cosmological redshift. There were several proposals in terms of photon-photon or photon-matter interaction due to some quantum effects (e.g., Finley-Freundliech 1954; Pecker et al. 1972; Laio et al. 1997; Moret-Bailly 2001). Potentially, this effect could explain the high redshifts of some anomalous redshift objects, since light travelling through their outer atmospheres could be redshifted before leaving it, and the blurring would not be a problem here since the distance travelled is short.

5.3.4. Variable mass hypothesis

Apart from the mechanisms given in the last subsection, non-standard physics has also been used to explain the redshift problem. Hoyle & Narlikar (1964) developed a new theory of gravitation with particle masses depending on time according to $m \sim t^2$ and redshifts

$$1 + z = \frac{\lambda_{source}}{\lambda_{observer}} = \frac{m_{observer}}{m_{source}}, \tag{18}$$

where "observer" and "source" stands for the measures from the different system at the Earth and in the source respectively. An explanation that these authors give for anomalous redshift galaxies is that new matter is being created there with $t = 0$, $m_{source} = m(t = 0)$ for that new matter and that the mass varies with the age (Narlikar 1977; Narlikar & Arp 1993) to produce different redshifts.

5.3.5. Higher redshift galaxies ejected by a parent galaxy?

Some proposed models (e.g., Arp 1999a,b; Arp & Russell 2001; Bell 2002a,b) assume that some QSOs are ejected by a parent galaxy and decrease in redshift as they move outward,

often although not always along the minor axis (the more recent ejections are near the axes, but they later move away because of peculiar motions, precession of the galaxy or the spin axis of the nucleus; Arp 1999b), until they reach a maximum distance of ~ 500 kpc when they fall back to the parent galaxy and turn into compact, active galaxies and, when they are older, into normal galaxies. Galaxies would beget galaxies; they would not be made from initial density fluctuations in a Big Bang Universe (Burbidge 1999b). It is usually claimed that the variable mass hypothesis is the explanation for the intrinsic redshifts. However, the scenario of "galaxies beget galaxies (with different redshift)" should be considered as a separate matter from the variable mass hypothesis or the Quasi Steady State Theory because other explanations of the redshifts and other cosmological scenarios could be compatible with the present idea.

This scenario seems to fit quite well the observed system: we would have three (or possibly only two or one, if we considered that some of the galaxies are background galaxies but not all of them) ejected together with the material of the filament, and we could think that any of the objects #21, #22 or #23 might be part of the ejection on the other side of the galaxy, or the QSO candidates whose spectra remains to be taken (#19, #36). The nearly coincidence of the redshifts of two of these objects with the redshifts of the HII galaxies in the filament make us think that they have likely a common interpretation: either objects with z=0.245 and z=0.246 and objects with z=0.394 and z=0.401 belong to the same two groups of galaxies respectively (in a cosmological redshift interpretation) or all of them are ejected by the parent galaxy NGC 7603 (in a non-cosmological redshift interpretation). Nevertheless, as said in §5.3.1, in the cosmological interpretation it would still remain to explain the low value of P. Therefore, if we want to avoid the word "coincidence" in all aspects (positions and redshifts) we must assume that all objects (#1, #2, #22, #23) are ejected by the parent galaxy.

HST images might show the interaction of the filament with objects #1 and #2 (see §3.2.1). The narrow line character in these objects (in principle, classified as HII galaxies according to their line ratios) would be a result of the ejection and interaction with the filament. Evidence is shown in other papers (e.g., Keel et al. 1998, 1999; Arp 1999a; Burbidge et al. 2003) that when QSOs interact with ambient material they become less compact and had narrower lines emitted from more a more diffuse body. This could be the physical explanation. Dynamically disturbed starburst galaxies, as illustrated by the case of NGC 2777 (Arp 1988), tend to be the small companions of larger nearby galaxies belonging to older stellar populations. According to Arp (1988), they are recently created galaxies in which star formation is stimulated by recent ejection from the parent galaxy; some older stars, together with stellar material, are suggested to be removed from the larger galaxy in the course of this ejection. In the system NEQ3 near NGC4151, a QSO and an HII-galaxy have almost identical redshifts, with a separation of 2.8 arcseconds and nearly the same magnitudes; the HII-galaxy is embedded in a filament while the

QSO is a little bit further away (Gutiérrez & López-Corredoira, in preparation). It is another example of environment where QSOs and narrow emission line galaxies have some relation. Therefore, the established fact of observing narrow emission line galaxies instead of QSOs is also contemplated in the theory, although the analysis of QSO-galaxy associations is more frequent. The origin of these sources, through the interaction, would also explain the high observed equivalent width in their Hα lines.

According to this theory, the intrinsic redshifts are indicated to evolve in discrete steps as the QSOs evolve into galaxies (Arp 1999b). The peaks in the quantization of the redshifts would be at redshifts around 0.06, 0.30, 0.60, 0.96, 1.41, 1.96 (Arp et al. 1990; Burbidge & Napier 2001), although the dispersion is large mainly because of peculiar velocities.

The redshifts of the HII-galaxies suggest a possible relation in pairs of objects: the pair in the filament with redshifts 0.245 and 0.394 could stem from the same original source with intrinsic redshift ≈ 0.32 (the exact value of this number indeed depends on the respective masses of the HII-galaxies), and a superposed Doppler radial velocities of around $\pm$17000 km/s, for instance (velocities of this order are obtained by Bell 2002a). A similar pair might be the HII-galaxies at 0.246 and 0.401 away from the filament, on the other side of NGC 7603, but these might be well in the background. This value of $z \approx 0.32$ (around $z \approx 0.28$ for an observer at NGC 7603) is close to the peak in the periodicity of QSOs/galaxies of $z = 0.30$ (Arp et al. 1990; Burbidge & Napier 2001). The same argument might be applicable to the pair of objects #22-#23. The emission in pairs or triplets could be very common according to this theory. Bell (2002a,b) proposes that the ejection occurs in triplets along the rotation axis of the central torus, and that these triplets are composed of a singlet and a pair that simultaneously separate in opposite directions and at 90° to the triplet ejection direction. The separation between the singlet and the pair is higher than the pair separation; if this were the case in NGC 7603, we would have to find the singlets somewhere in the field of NGC 7603.

There is no unique representation of the system in terms of this theory of ejection. We do not have enough information about the distances of the sources with respect to the parent galaxy to build an unique 3-D representation. For instance, Fig. 8 represents a possible configuration according to the ejection theory. The inclination of the galaxy is around 20 degrees with respect the line of sight (ellipticity ≈ 0.35), so slight deviations of the objects from the rotation axis could produce the projected image that we have observed. Figure 8 shows a model in which the filament is not in the plane of the galaxy, but is ejected in a direction nearly perpendicular to the plane.

The filament does not have a blue colour like the other spiral arms in NGC 7603; neither does it have young star formation since it has no emission lines (paper I); instead, it has a red colour (see Fig. 3), like the old population of the disc of NGC 7603. Therefore, the filament could possibly be some material stripped from the main galaxy as a result

of some tidal interactions or ejection. A reason for the visibility of the filament in this ejection with 24.0 mag/arcsec^2, while is not observed in other systems, might be the integration along the line of sight of a filament that is nearly tangential to the line of sight and provides a high column density. Nonetheless, as has been said, there are some other cases which also have similar continuous or nearly-continuous filaments/arms (with some gaps) connecting different-redshift objects (see §5.2.2). Perhaps NGC 7603 is the clearest case, but it may not be unique.

The other side of NGC 7603 (behind NGC 7603 if we assume that the filament and its ejected objects are in front of it) could also have some ejected objects. We do not see the filament there, possibly because it is behind the galaxy.

Other possible scenario within this ejection hypothesis would be that all the galaxies are in the plane of NGC 7603. It is noteworthy that all the five HII galaxies and NGC 7603B are almost aligned, which could lead us to think of an ejection along some common axis. However, this axis would not be the rotation axis, which is the expected axis in ejection theories.

6. Summary

- We present new observations in the field of the Seyfert galaxy NGC 7603. These comprise broad and narrow band imaging, and intermediate resolution spectroscopy of several objects in the field.
- We have delineated the halo around NGC 7603 out to the isophote 26.2 mag/arcsec^2 in the Sloan r band filter finding several signs of irregularities and asymmetries towards the east. Neither these eastern asymmetries nor the filament towards the east, apparently connecting NGC 7603 and NGC 7603B, can be easily understood in an isolated galaxy, and until now no good candidates of companions on the east side of NGC 7603 with the same redshift have been found.
- With improved spectra with respect to those published in Paper I, we have confirmed the redshift of the two objects in the filament connecting NGC 7603 and NGC 7603B and we have observed their $H\alpha$ lines for the first time.
- The better resolution achieved in these new spectra and HST imaging of these objects have allowed their more accurate classification as HII galaxies. We have not detected any signs of variability in these objects at levels $\geq 0.3 - 0.4$ mag. We found very strong star formation (or whatever the cause of the high equivalent widths of Hα lines) in both of them and the HST images show some distortions in the shape of both galaxies, which might suggest an interaction with the filament.
- We have detected new narrow emission line galaxies at z =0.246, 0.117 and 0.401, 0.8, 1.5, 1.7 minutes to the West of the filament between NGC 7603 and NGC 7603B. The nearly coincidence of the redshifts of two of these objects with the redshifts

of the HII galaxies in the filament make us think that they have likely a common interpretation: either objects with z=0.245 and z=0.246 and objects with z =0.394 and z =0.401 belong to the same two groups of galaxies respectively (in a cosmological redshift interpretation) or all of them are ejected by the parent galaxy NGC 7603 (in a non-cosmological redshift interpretation).

– The probability of a fortuitous accumulation of objects as bright as NGC 7603, NGC 7603B, and the two objects in the filament has been computed resulting in $\sim 3\times10^{-9}$. The (possible, although not sure) detection of vigorous star formation observed in the HII-galaxies of the filament, if confirmed, would have a probability 2×10^{-4} giving a total probability $\sim 6 \times 10^{-13}$. They look dwarf HII-galaxies (non-cosmological redshift) rather than normal/giant HII-galaxies (cosmological redshift).

– An explanation in terms of cosmological redshifts (with or without gravitational lensing, with or without clusters in the line of sight has very low probability although it is not impossible. Alternative explanations have been analysed.

Acknowledgments: Thanks are given to the referee Jack Sulentic for useful comments and criticisms on the interpretations of probabilities. We thank also to Evencio Mediavilla (IAC) who read the manuscript and gave helpful comments. This research has made use of the SIMBAD database, operated at CDS, Strasbourg, France.

References

Arp, H. C. 1971, ApL, 7, 22

Arp, H. C. 1975, PASP, 87, 545

Arp, H. C. 1980, ApJ 239, 469

Arp, H. C. 1981, ApJ 250, 31

Arp, H. C. 1987, QSOs, Redshifts and Controversies, Berkeley: Interstellar Media

Arp, H. C. 1988, in: High energy astrophysics: Supernovae, remnants, active galaxies, cosmology, Springer-Verlag, Berlin, 1988, p. 160

Arp, H. C. 1998, Seeing red: redshifts, cosmology and academic science Montreal: Apeiron

Arp, H. C. 1999a, ApJ 525, 594

Arp, H. C. 1999b, Active Galactic Nuclei and Related Phenomena, Y. Terzian, E. Khachikian and D. Weedman, S. Francisco: Astronomical Society of the Pacific, 347

Arp, H. C., Bi, H., Chu, Y., & Zhu, X. 1990, A&A 239, 33

Arp, H. C., Burbidge, E. M., Chu, Y., Flesch, E., Patat, F., Rupprecht, G. 2002, A&A 391, 833

Arp, H. C., Burbidge, E. M., Chu, Y., & Zhu, X. 2001, ApJ, 553, L11

Arp, H. C., & Russell, D. A. 2001, ApJ 549, 802

Baryshev, Y. V., & Bukhmastova, Y. L. 1997, Astron. Reports 41, 436

Bell, M. B. 2002a, ApJ, 566, 705

Bell, M. B. 2002b, ApJ, 567, 801

Benítez, N., Sanz, J. L., and Martínez-González, E. 2001, MNRAS , 320, 241

Bennett, C. L., Halpern, M., Hinshaw, G., et al. 2003, ApJ, accepted. Preprint astro-ph/0302207

Bertin, E., & Arnouts, S. 1996, AAS, 117, 393

Biviano, A., Katgert, P., Mazure, A., Moles, M., den Hartog, R., Perea, J., Focardi, P. 1997, A&A 321, 84

Boyle, B. J., Jones, L. R., Shanks, T., 1991, MNRAS 251, 482

Boyle, B. J., Shanks, T., Croom, S. M., Smith, R. J., Miller, L., Loaring, N., & Heymans, C. 2000, MNRAS, 317, 1014

Bukhmastova, Y. L. 2001, Astron. Reports 45, 675

Bukhmastova, Y. L. 2003, Astron. Letters 29, 214

Burbidge, G. R. 1996, A&A, 309, 9

Burbidge, G. R. 1999a, ApJ, 511, L9

Burbidge, G. R., 1999b, in: Cosmological Parameters and the Evolution of the Universe, K. Sato, Dordrecht: Kluwer, p. 286

Burbidge, G. R. 2001, PASP, 113, 899

Burbidge, E. M., Burbidge, G. R., Arp, H. C., Zibetti, S. 2003, ApJ 591, 690

Burbidge, G. R., Hoyle, F., & Schneider, P. 1997, A&A, 320, 8

Burbidge, G. R., Napier, W. 2001, AJ 121, 21

Carilli, C. L., & van Gorkom, J. H. 1992, ApJ, 399, 373

Carilli, C. L., van Gorkom, J. H., & Stocke, J. T. 1989, Nature, 338, 134

Carter, B. J., Fabricant, D. G., Geller, M. J., & Kurtz, M. J. 2001, ApJ 559, 606

Croom, S. M., Smith, R. J., Boyle, B. J., Shanks, T., Loaring, N. S., Miller, L., & Lewis, I. J. 2001, MNRAS 322, L29-L36

Datta, S., Roy, M., & Moles, M. 1998*a*, Inst. Journ. Theor. Phys.,, 37, 1313

Datta, S., Roy, M., & Moles, M. 1998*b*, Inst. Journ. Theor. Phys.,, 37, 1469

de Ruiter, H. R., Fan ti, R., Parma, P., Lub, J., Morganti, R., & Ekers, R. D. 1998, MNRAS, 337, 711

Dessauges-Zavadsky, M., Pindao, M., Maeder, A., & Kunth, D. 2000, A&A 355, 89

Dressler, A., Thompson, I. B., Shectman, S. A. 1985, ApJ 288, 481

de Vaucouleurs, G., de Vaucouleurs, A., Corwin JR., H. G., Buta, R. J. Paturel, G.,& Fouque, P. 1991, Third Reference Catalogue of Bright Galaxies. . Springer-Verlag. N.Y.

Ellis, R., Santos, M. R., Kneib, J. P., & Kuijken, K. 2001, ApJ, 560, L119

Filippenko, V. A., & Terlevich, R. J. 1992, ApJ 397, L79

Finley-Freundlich, E., 1954, Phil. Mag. 45, 303

Gallagher, S. C., Charlton, J. C., Hunsberger, S. D., Zaritsky, D., & Whitmore, B. C. et al. 2001, AJ, 122, 163

Gaztañaga, E. 2003, ApJ 589, 82

Gibson, C. H. 1996, Appl. Mech. Rev. 49, 299

Gibson, C. H., & Schild, R. E. 2003, AJ, submitted. Preprint astro-ph/0304107

Gisler, G. R. 1978, MNRAS 183, 633

Goodrich, R. W. 1989, ApJ 340, 190

Gott, J. R., III, & Gunn 1974, ApJ, 190, L105

Gutiérrez, C. M., López-Corredoira, M., Prada, F., & Eliche M. C. 2002, ApJ, 579, 592

Hickson, P. 1982, ApJ 255, 382

Hoyle, F. 1972, Henry Norris Russel Lecture, The Seattle Meating of the AAS

Hoyle, F., & Burbidge, G. R. 1996, A&A, 309, 335

Hoyle, F., Burbidge, G., & Narlikar, J. V. 1993, ApJ, 410, 437

Hoyle, F., & Narlikar, J. V., 1964, Proy. Roy. Soc. London A282, 191

Jain, B., Scranton, R., Sheth, R. K. 2003, preprint astro-ph/0304207

Johnston, K. V., Sackett, P. D., & Bullock, J. S. 2001, ApJ 557, 137

Keel, W. C., Cohen, S. H., Windhorst, R. A., & Waddington, I. 1999, AJ 118, 2547

Keel, W. C., Windhorst, R. A., Cohen, S. H., Pascarelle, S., & Holmes, M. 1998, NOAO Newsletter 53, 1

Kennicutt, R. C. Jr., Tamblyn, P., & Congdon C. W. 1994, ApJ 435, 22

Kollatschny, W., Bischoff, K., & Dietrich, M. 2000, A&A, 361, 901

Kondratko, P. T., Greenhill, L. J., Moran, J. M. 2001, AAS 199, 5101

Kopylov, I. M., Lipovetskii, V. A., Pronik, V. I. & Chuvaev, K. K. 1974, Afz, 10, 483

Laio, A., Rizzi, G., & Tartaglia, A. 1997, Phys. Rev. E 55, 7457

Landolt, A. U. 1992, A&A, 104, 340

Lisenfeld, U., Braine, J., Duc, P.-A., Leon, S., Charmandaris, V., and Brinks, E. 2002, A&A 394, 823

López-Corredoira, M., & Gutiérrez, C. M. 2002, A&A 390, L15 (Paper I)

Malkan, M. A., Gorjian, V., & Tam, R. 1998, ApJS 117, 25

Maoz, D., Koratkar, A., Shields, J. C., et al. 1998, AJ 116, 55

Mathis, J. S. 1990, ARA&A 28, 37

Mendes de Oliveira, C., 1995 MNRAS 273, 139

Metcalfe, N., Shanks, T., Fong, R., & Jones, L. R. 1991, MNRAS, 249, 498

Meyer, M. J., Drinkwater, M. J., Phillips, S., & Couch, W. J. 2001, MNRAS, 324, 343

Moles, M. Marquez, I., & Sulentic, J. W. 1998, A&A, 334, 473

Moret-Bailly J., 2001, preprint astro-ph/0110525

Narlikar, J. V., 1977, Ann. Phys. 107, 325

Narlikar, J. V. 1989, Space Science Reviews, 50, 523

Narlikar, J. V., & Arp, H. C., 1993, ApJ 405, 51

Noerdlinger, P. D. 1975, ApSS 38, 457

Ohyama, Y., Taniguchi, Y., Hibbard, J. E., & Vacca, W. D. 1999, AJ 117, 2617

Pecker, J. C., Roberts, A. P., & Vigier, J. P. 1972, Nature 237, 227

Pietsch, W., Vogler, A., Kahabka, P., Jain, A., & Kelin, V. 1994, A&A 284, 386

Rose, J. A., Gaba, A. E., Caldwell, N., & Chaboyer, B. 2001, AJ 121, 793

Roy, S., Kafatos, M., Datta, S. 2000, A&A, 353, 1134

Schlegel, D. J., Finkbeiner, D. P., & Davis, M. 1998, ApJ 500, 525

Schombert, J. M., Wallin, J. F., & Struck-Marcell, C. 1990, AJ 99, 497

Schneider, P. 1989, A&A 221, 221

Sharp, N. A. 1986, ApJ, 302,245

Sluse, D., Surdej, J., Claeskens, J. F., de Rop, Y., Lee, D. W., Iovino, A., & Hawkins, M. R. S. 2003, A&A 397, 539

Smith, J. A., Tucker, D. L., Kent S., et al. 2002, AJ 123, 2121

Stockton, A., & Ridgway, S. E. 1998, AJ 115, 1340

Sulentic, J. W. 1997, ApJ 482, 640

Sulentic, J. W., & Arp, H. C. 1987, ApJ 319, 687

Sulentic, J. W., Marziani, P., Zamanov, R., Bachev, R., Calvani, M., Dultzin-Hacyan, D. 2002, ApJ 566, L71

Sulentic, J. W., Rosado, M., Dultzin-Hacyan, D., Verdes-Montenegro, L., Trinchieri, G., Xu, C., & Pietsch, W. 2001, AJ 122, 2993

Sulentic, J. W., Zwitter, T., Marziani, P., Dultzin-Hacyan, D. 2000, ApJ 536, L5

Telles, E., & Terlevich, R. 1995, MNRAS 275, 1

Teplitz, H. I., Collins, N. R., Gardner, J. P., Hill, R. S., Heap, S. R., Lindler, D. J., Rhodes, J., & Woodgate, B. E. 2003, ApJS 146, 209

Tohline, J. E., & Osterbrock, D. E. 1976, Lick Obs. Bull., 742, 1

Veilleux, S., Osterbrock, D. E. 1987, ApJS 63, 295

Williams, B. A., Yun, M. S., & Verdes-Montenegro, L. 2002, AJ 123, 2417

Wolf, E. 1986, Phys. Rev. Lett., 56, 1379

Wu, X. P. 1996, Fund. Cosmic Physics 17, 1

Appendix A: Cumulative counts of galaxies and QSOs

The cumulative counts of galaxies in the B-band can be derived from differential galaxy counts from Metcalfe et al. (1991) for galaxies between $20.5 < B < 24.5$ (magnitudes corrected for extinction):

$$\log N(B_0 - 0.25 < B < B_0 + 0.25)$$

$$= 0.494 B_0 - 7.72 \text{ deg}^{-2}. \quad \text{(A.1)}$$

The cumulative count is:

$$N(B < B_{lim}) \approx 2 \int_{-\infty}^{B_{lim}} dB_0 N(B_0 - 0.25 < B < B_0 + 0.25)$$

$$= 3.35 \times 10^{-8} \times 3.12^{B_{lim}} \text{ deg}^{-2}. \quad \text{(A.2)}$$

This assumes as an approximation that eq. (A.1) applies for $B_0 < 20.5$, which is more or less correct because the change of slope is very small for lower magnitudes.

The cumulative QSO counts are given by:

$$N(b_j < b_{j,lim}) \approx 1981 - 214.2 b_{j,lim} + 5.792 b_{j,lim}^2 \text{ deg}^{-2}. \quad \text{(A.3)}$$

We derived this expression by fitting the cumulative QSO counts in the photographic b_j filter from the survey by Boyle et al. (2000), based in a multicolour selection of QSOs. Fig. 9 shows that fit. The Boyle et al. (2000) data are for $b_j < 21.0$, but we extrapolate the fit (A.3) as an approximation to higher magnitudes. Another point obtained from a spectroscopic survey of faint QSOs (Boyle et al. 1991) confirms that the fit and its

extrapolation are reasonably good (see Fig. 9). There are some uncertainties in these estimates but they are low. One major concern is whether these QSO counts are complete, and we know that they are quite complete. The multicolour selection of QSOs is complete for QSOs of redshift of $z < 2.2$ (90%), or 80% for $z > 2.2$ (Boyle et al. 2000; Meyer et al. 2001). There is no selection effect that could favour the statistics: only $10-15\%$ of extra QSOs which are not included in these counts.

FIGURES

1. A grey scale and contour image in the R band of the region around the galaxy NGC 7603. The contours correspond to isophotes 24.8, 25.3 and 26.2 mag/arcsec^2.
2. A grey-scale R band image and contours corresponding to Hα emission at the redshift of the galaxy NGC 7603.
3. Sloan g-r colour of NGC7603. From bluer to redder colours [lower to higher values of (g-r)]: black-blue-green-red-white. The center of NGC 7603 is saturated. Noteworthy aspects are the red colour of an asymmetrical strip crossing NGC 7603, the young population (blue) at the north of NGC 7603 and the average (green) colour of of the filament connecting NGC 7603 and NGC 7603B.
4. Position of the sources in table 2 (only sources with $m_u \leq 23.8$ except source #1; NGC 7603 and NGC 7603B not included). With the double circle, we point out the three sources which follow eq. (1), candidate QSOs by the multicolour selection. Dot-dashed lines represent the position of the three long slits placed in the field of NGC 7603 to obtain the spectra of some objects.
5. Diagrams colour-apparent magnitude and colour-colour of objects that were selected in the field of NGC 7603 (table 2). The square represents object #2. Object #1 is not in the plots because we have not its u magnitude. The lines indicate the limits of (g-r) colour under which QSOs are likely to be found (see §3.2): there are 3 candidates with (g-r) under the red line.
6. HST image in the F606W filter of the region centred on the filament between NGC 7603 and NGC 7603B. Also shown are the contours of the two objects in the filament. Note that there are many bad pixels/cosmic rays in the images that do not correspond to any object. The PSF is $\sim$ 0.1 arcsec. Dotted lines show the area (around 140 arcsec^2) that we consider "filament" for the calculation of the probabilities in §5.2.2.
7. Main spectral features (corrected of redshift) of objects #1 ($z = 0.245$, in the filament), #2 ($z = 0.394$, in the filament), #21 ($z = 0.117$), #23 ($z = 0.246$) and #22 ($z = 0.401$). Dashed lines below the spectra are their zero-flux levels.
8. Possible representation of the system of NGC 7603/NGC 7603B/Object #1/Object #2 if we accept the hypothesis of the three last objects to be ejected by the parent galaxy, NGC 7603. The inclination of NGC 7603 with respect the line of sight is $\approx 20^\circ$. The major axis in the projected image (Axis 1) has a position angle $\approx -15^\circ$; the minor axis in the projected image is "Axis 2".
9. Cumulative QSO counts data (Boyle et al. 2000; 1991) and a fit of a second polynomial degree to the Boyle et al. (2000) data.

This figure "f1.jpg" is available in "jpg" format from:

http://arxiv.org/ps/astro-ph/0401147v1

This figure "f2.jpg" is available in "jpg" format from:

http://arxiv.org/ps/astro-ph/0401147v1

This figure "f3.jpg" is available in "jpg" format from:

http://arxiv.org/ps/astro-ph/0401147v1

This figure "f4.jpg" is available in "jpg" format from:

http://arxiv.org/ps/astro-ph/0401147v1

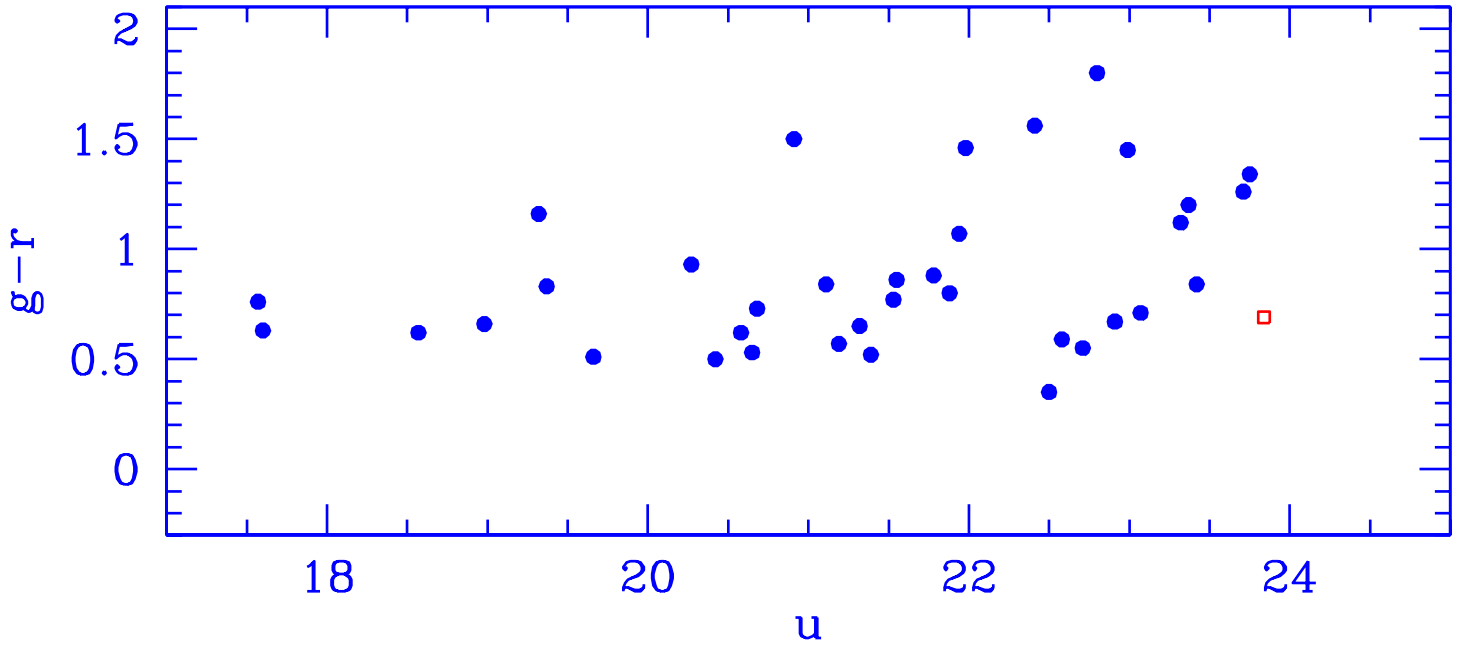
2
1.5
1
0.5
0
g−r
18
20
22
24
u

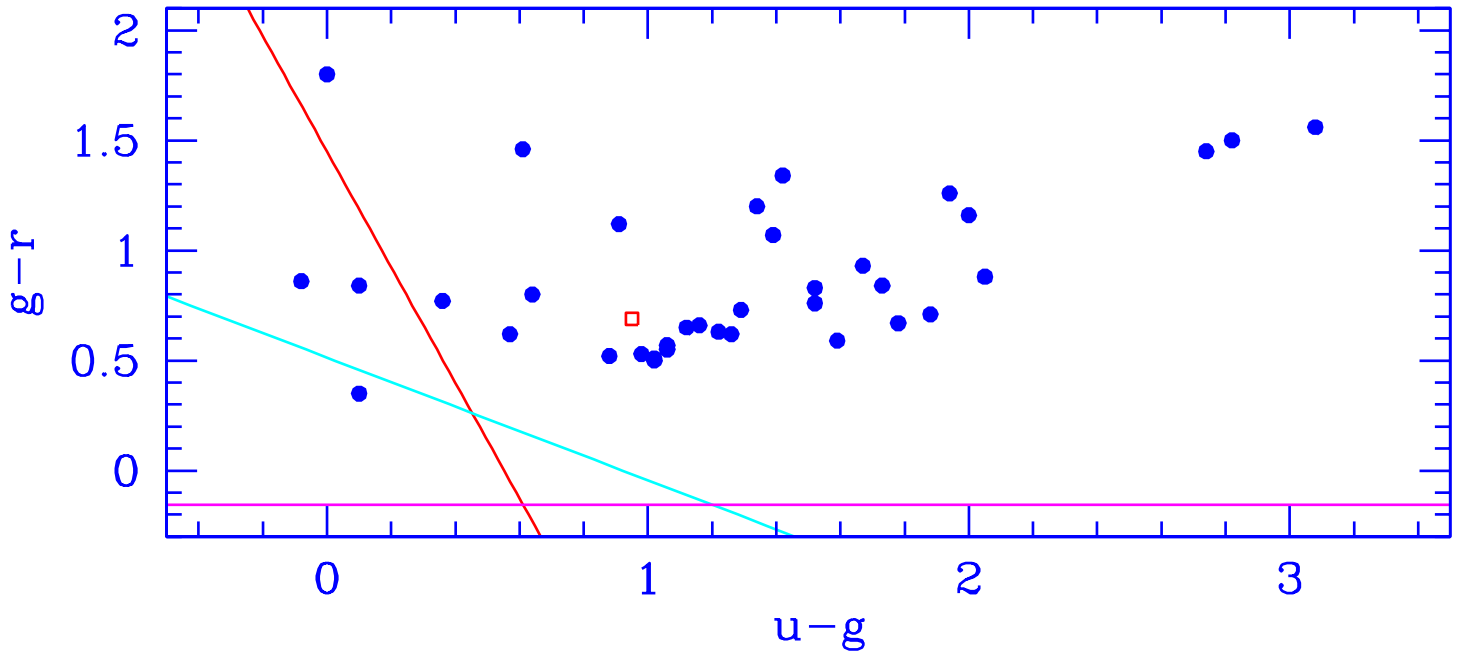
2
1.5
1
0.5
0
g−r
0
1
2
3
u−g

This figure "f6.jpg" is available in "jpg" format from:

http://arxiv.org/ps/astro-ph/0401147v1

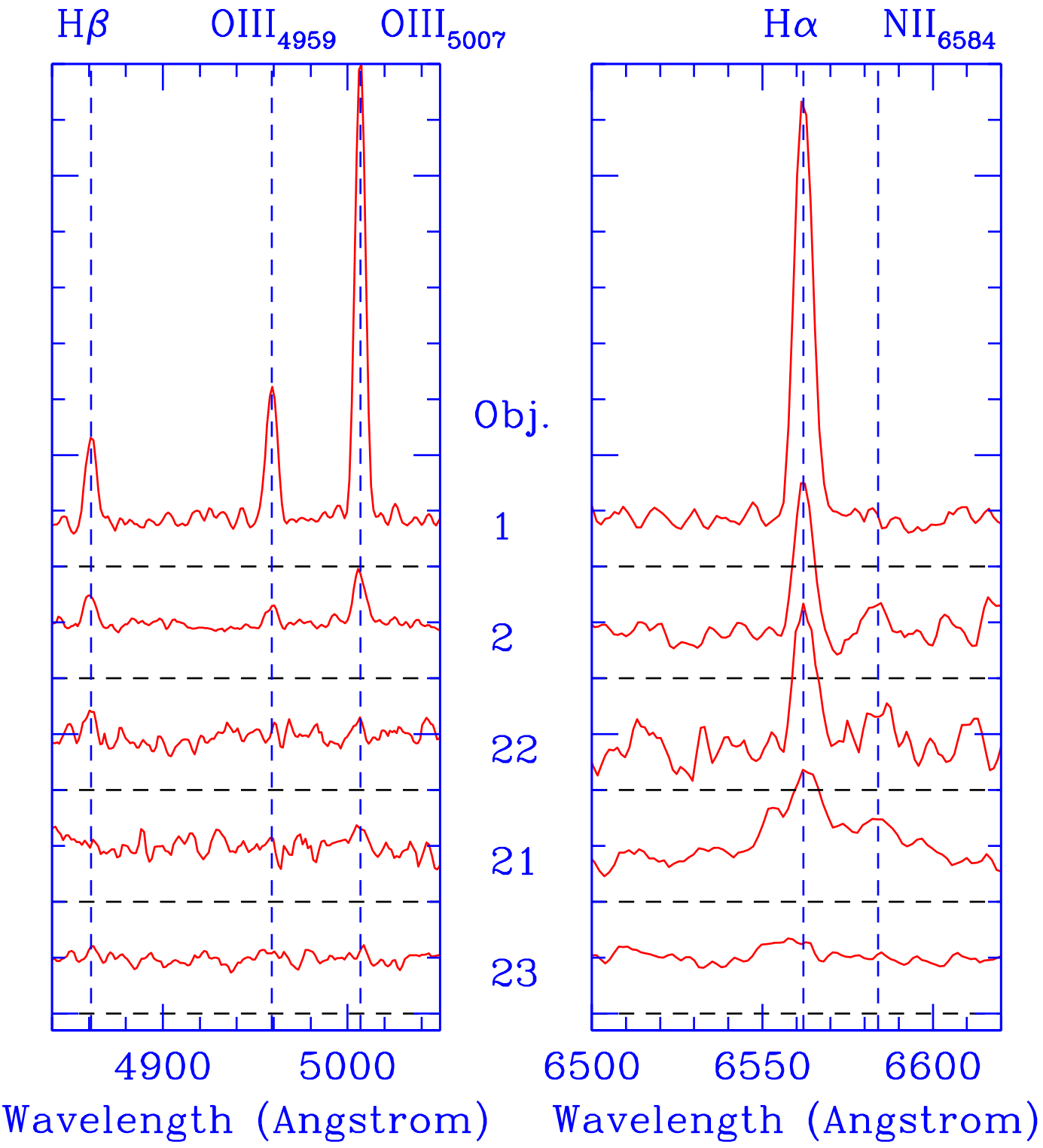
Hβ
OIII4959
OIII5007
Hα
NII6584
Obj.
1
2
22
21
23
4900
5000
6500
6550
6600
Wavelength (Angstrom)
Wavelength (Angstrom)

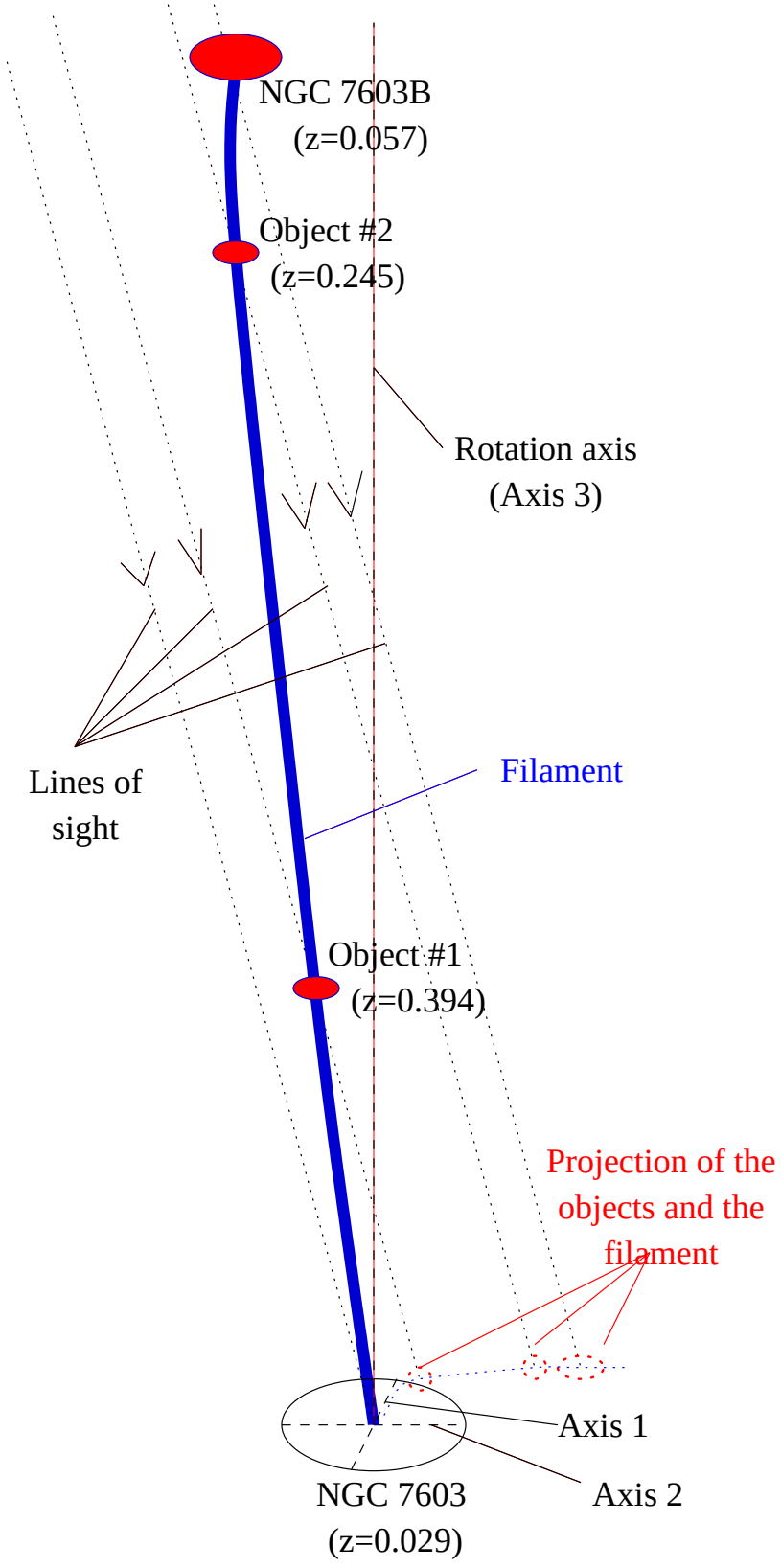
NGC 7603B
(z=0.057)
Object #2
(z=0.245)
Rotation axis
(Axis 3)
Lines of
sight
Filament
Object #1
(z=0.394)
Projection of the
objects and the
filament
Axis 1
Axis 2
NGC 7603
(z=0.029)

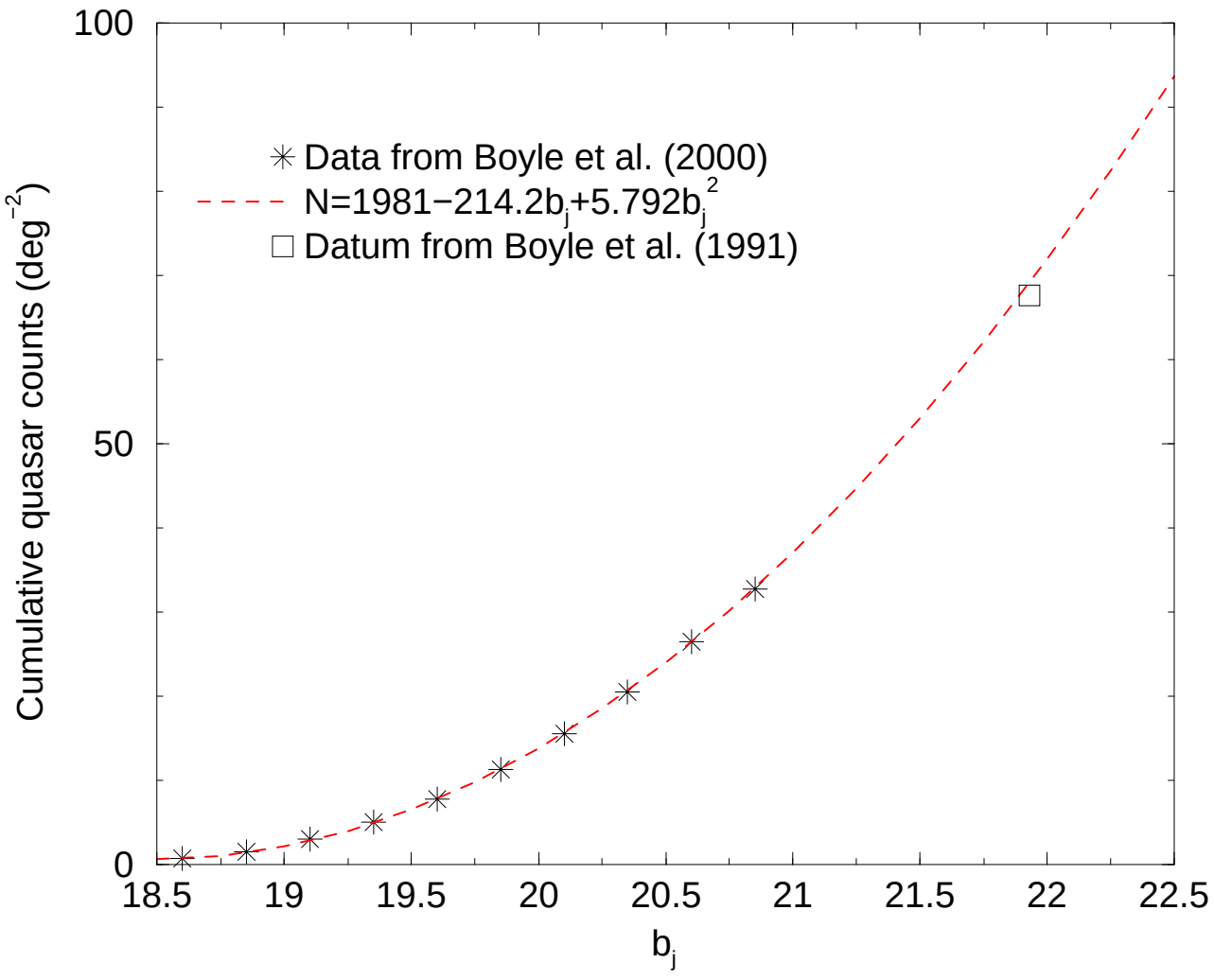
100
50
0
18.5
19
19.5
20
20.5
21
21.5
22
22.5
Cumulative quasar counts (deg^{-2})
b_j
Data from Boyle et al. (2000)
N=1981−214.2b_j+5.792b_j^2
Datum from Boyle et al. (1991)